Bioorganic Chemistry 173 (2026) 109651

Contents lists available at ScienceDirect

Bioorganic Chemistry

journal homepage: www.elsevier.com/locate/bioorg

A novel antimicrobial peptide Anguinin$_{55–72}$ identified from *Anguilla japonica* exhibiting protection against *Edwardsiella tarda* infection

Wenbin Zheng [a,b], Fangyi Chen [a,b,c,*], Wenhao Yu [a,b], Tingting Gao [a,b], Ziyuan Yan [a,b], Yuqi Bai [a,b], Hang Sun [a,b], Ke-Jian Wang [a,b,c,*]

[a] State Key Laboratory of Marine Environmental Science, College of Ocean & Earth Sciences, Xiamen University, Xiamen 361102, China
[b] State-Province Joint Engineering Laboratory of Marine Bioproducts and Technology, College of Ocean & Earth Sciences, Xiamen University, Xiamen 361102, China
[c] Marine Biological Antimicrobial Peptide Industry Research Institute, Fujian Ocean Innovation Center, Xiamen 361102, China

ARTICLE INFO

Keywords:
Anguilla japonica
Antimicrobial peptide
Anguinin$_{55–72}$
Antimicrobial activity
Edwardsiella tarda challenge

ABSTRACT

Edwardsiella tarda poses a substantial threat to fish populations, inducing severe systemic infections, especially pronounced in economically valuable species such as the Japanese eel (*Anguilla japonica*). Current therapeutic options are limited, and the emergence of multidrug-resistant strains further underscores the urgent need to develop novel antimicrobial alternatives. Antimicrobial peptides present promising alternatives because of their extensive activity range and minimal potential for resistance development. In this study, we identified a novel functional gene from *A. japonica*, named *Anguinin*, which encodes a mature peptide comprising 99 amino acids. The *Anguinin* gene was broadly expressed in various tissues of healthy *A. japonica* and showed significant induction in immune-related tissues following *E. tarda* infection. A truncated peptide, Anguinin$_{55–72}$, derived from this gene, exhibited potent antimicrobial properties against a wide range of pathogens. Mechanistic studies revealed that Anguinin$_{55–72}$ disrupted bacterial membranes, increased membrane permeability, and triggered the accumulation of reactive oxygen species, ultimately causing bacterial death. The peptide also demonstrated antibiofilm activity and maintained stability at high temperatures without cytotoxicity. The *in vivo* animal models were constructed using zebrafish and Japanese eels infected with *E. tarda*. The results showed that Anguinin$_{55–72}$ significantly increased survival rates of *Danio rerio* and *A. japonica*. Additionally, in the Japanese eel model, Anguinin$_{55–72}$ significantly reduced disease severity, decreased bacterial loads, downregulated the expression of pro-inflammatory cytokines and promoted the recovery of tissue lesions. Taken together, Anguinin$_{55–72}$ holds promise as an alternative to conventional antibiotics for controlling *E. tarda* infections in aquaculture to address the challenge of escalating antibiotic resistance.

1. Introduction

Edwardsiella tarda is a facultative anaerobic, Gram-negative bacterium that can cause a serious disease in fish known as Edwardsiellosis [1]. This disease manifests itself in fish in a variety of ways, including septicemia, hepatonephritis, eel ulcer disease, and eel hepatonephro syndrome. It has been reported in economically important fish species globally, such as Japanese eel (*Anguilla japonica*) [2,3], tilapia (*Oreochromis niloticus*) [4], red snapper (*Pagrus major*) [5], turbot (*Scophthalmus maximus*) [6], and channel catfish (*Ictalurus punctatus*) [7], causing considerable harm to aquaculture. Septicemia, in particular, has led to substantial mortality rates (up to 70%) and significant economic losses in both freshwater and marine aquaculture animals worldwide [8]. Over the past decades, despite the progress made in research on Edwardsiellosis and the development of several effective vaccine candidates, they are still not yet commercially available for large-scale use. Consequently, the primary measures for the prevention and control of Edwardsiellosis remains to be the application of antibiotics, including cephalosporins, ampicillin, aminoglycosides, and fluoroquinolones [1,9].

Admittedly, antibiotics have been instrumental in advancing aquaculture and animal husbandry since the discovery of penicillin by Alexander Fleming in 1928 [10]. They are extensively employed to treat illnesses caused by microbial infections. In addition, antibiotics are also

* Corresponding authors at: State Key Laboratory of Marine Environmental Science, College of Ocean & Earth Sciences, Xiamen University, Xiamen, Fujian 361102, China.
E-mail addresses: chenfangyi@xmu.edu.cn (F. Chen), wkjian@xmu.edu.cn (K.-J. Wang).

https://doi.org/10.1016/j.bioorg.2026.109651
Received 12 December 2025; Received in revised form 28 January 2026; Accepted 12 February 2026
Available online 19 February 2026

widely employed to improve the growth and productivity of livestock, leading to a rapid increase in their usage. However, the widespread use and frequent misuse of antibiotics has given rise to a serious problem of microbial resistance, resulting in treatment failures, increased incidence and mortality, as well as higher healthcare costs [11]. The use of antibiotics in non-human animals, particularly in agriculture and aquaculture, significantly contributes to the development of resistance that impacts on humans [12]. Based on a comprehensive global analysis of antimicrobial resistance, it is projected that over 39 million individuals may succumb to infections with antibiotic-resistant pathogens from the present until 2050 [13]. Therefore, decreasing antibiotic usage is crucial to curb the rise and dissemination of antibiotic-resistant bacteria in the environment, throughout the food chain and in animals, and ultimately reducing the corresponding public health risks [14]. Concurrently, it is imperative to explore and develop effective alternatives to conventional antibiotics.

Antimicrobial peptides (AMPs), hailed by scientists as "natural antibiotics", emerge as highly promising natural substitutes for traditional antibiotics [15]. They play a crucial role in the innate immune system and exhibit a wide range of efficacy against bacteria, fungi, and viruses. Moreover, they also help to regulate immune responses and perform various other biological functions [16]. AMPs demonstrate their antibacterial effects through three main mechanisms: inhibiting cell wall synthesis and disrupting its integrity [17]; interacting with negatively charged microbial membrane to increase permeability, leading to membrane rupture and the leakage of cellular contents [18]; and by disrupting intracellular organelles and interfering with normal metabolic activities, resulting in bacterial death [19]. In addition, AMPs are characterized by rapid bactericidal action, high efficacy in synergy, and low propensity to induce resistance [20]. These properties make the application of AMPs in clinical medicine, the food industry, livestock farming, and aquaculture highly promising [21,22].

Interestingly, AMPs are ubiquitous across all forms of life and are important components of the innate immune system [23]. Fish, a major species of aquatic animals, have a specific immune system that produces antibodies, but the number of antibodies is limited and the maturation of lymphocytes is slow, and studies have confirmed that the innate immune system is crucial for their defense against pathogens [24]. The Japanese eel (*Anguilla japonica*) is an anadromous, carnivorous fish widely distributed in freshwater habitats of the Western Pacific. Its life cycle involves six stages, requiring it to move from the ocean to rivers and then back to the ocean. This unique life cycle may require it to increase its reliance on innate immune effectors, making it a valuable resource for discovering novel AMPs. To date, only eight AMPs of Japanese eel have been reported, including AJN-10 [25], AjCath I (Cathelicidin family), Ajdefensin1 and Ajdefensin2 (β-defensin family), AJLEAP-2 (liver-expressed antimicrobial peptide 2), AJBPI-1 and AJBPI-2 (bactericidal/permeability increasing protein, BPI superfamily), and AJHbα [26]. Among them, only AJN-10 and AJHbα have antibacterial activity against *E. tarda*. However, the *in vivo* antibacterial efficacy of these AMPs against *E. tarda* remains to be determined. In recent years, the development of novel AMPs as potential alternatives to antibiotics for the treatment of pathogenic infections has garnered growing interest, but studies on AMPs related to diseases caused by *E. tarda* are still limited [27]. Therefore, it is of significant scientific importance to explore new AMPs in Japanese eel, which will help better understanding their immune defense mechanisms and provide a theoretical foundation for developing antimicrobial agents.

In this study, we identified a novel functional gene, named *Anguinin*, by analyzing the transcriptome database of *A. japonica* infected with *E. tarda*. The complete cDNA sequence of *Anguinin* gene was determined through RACE PCR, and its tissue distribution in healthy eels and its induced expression pattern following *E. tarda* infection were analyzed. Additionally, based on the physicochemical properties of Anguinin and the predictions of the AMP database, we screened and obtained a truncated peptide, Anguinin$_{55–72}$, with potential antimicrobial activity. It was chemically synthesized and the antimicrobial properties and underlying mechanism were determined. In turn, we initially investigated whether Anguinin$_{55–72}$ could exert *in vivo* effects using a model of zebrafish infected with *E. tarda* by examining the survival rate of the fish. Furthermore, we constructed a model of *E. tarda* infection in *A. japonica* to assess the anti-infective effects of Anguinin$_{55–72}$ by determining eel survival, disease-related indices, and bacterial clearance, as well as the effects on inflammation-related genes (including *IL-6*, *IL-8*, and *TNF-α*) using qPCR and liver tissue using HE staining. This study focuses on assessing the *in vitro* antimicrobial efficacy of the novel AMP Anguinin$_{55–72}$ and elucidating its role in combating *E. tarda* infection *in vivo*, which will provide a theoretical basis for the development of an effective antibacterial agent against *E. tarda* with a view to making it an alternative to antibiotics in future aquaculture.

2. Materials and methods

2.1. Animals, strains, and cell lines

Japanese eels (30 ± 5 g) were sourced from a wholesale aquatic products farm in Nansha District, Guangzhou City, China. They were acclimated in a constant-temperature circulation system of 28 °C with continuous oxygenation for more than seven days. Healthy Japanese eels were then dissected to collect samples of various tissues, including the brain, heart, spleen, gills, intestines, skin, stomach, muscle, liver, and trunk kidney.

The AB strain of standard zebrafish (*Danio rerio*), weighing about 0.5 g, were purchased from the China Zebrafish Resource Center in Wuhan, China. The zebrafish were housed in a controlled freshwater system with a temperature range of 26 °C–28 °C and were provided with brine shrimp twice daily. Prior to injection, the fish were tranquilized using a 60 mg/L solution of ethyl 3-aminobenzoate methanesulfonate (MS222, Sigma-Aldrich, USA).

The HEK293T cell line, obtained from the National Collection of Authenticated Cell Cultures in Shanghai, China, was maintained in DMEM medium (Gibco, USA) containing 10% fetal bovine serum (FBS) (Gibco, USA) at 37 °C in an atmosphere of 5% CO_2 incubator. Additionally, the zebrafish embryonic fibroblast cell line (ZF4), procured from the China Zebrafish Resource Center in Wuhan, China, was grown in a DMEM-F12 (1:1) medium (Gibco, USA) containing 10% FBS (Gibco, USA), and incubated at 28 °C under 5% CO_2.

The bacterial strains employed in this study were procured from the China General Microbiological Culture Collection Center (CGMCC), which included *Enterococcus faecium* (CGMCC NO. 1.131), *Listeria monocytogenes* (CGMCC NO. 1.10753), *Staphylococcus epidermidis* (CGMCC NO. 1.4260), *Staphylococcu saureus* (CGMCC NO. 1.2465), *Acinetobacter baumannii* (CGMCC NO. 1.6769), *Pseudomonas fluorescens* (CGMCC NO. 1.3202), *Pseudomonas putida* (CGMCC NO. 1.1836), *Escherichia coli* (CGMCC NO. 1.2389), *Pseudomonas aeruginosa* (CGMCC NO. 1.2421), *Vibrio harveyi* (CGMCC NO. 1.1593), *Vibrio alginolyticus* (CGMCC NO. 1.1833), *Vibrio parahaemolyticus* (CGMCC NO. 1.1997), *Vibrio fluvialis* (CGMCC NO. 1.1609), *Edwardsiella tarda* (CGMCC NO. 1.1872), *Crytococcus neoformans* (CGMCC NO. 2.1563), *Fusarium solani* (CGMCC NO. 3.5840), *Aspergillus niger* (CGMCC NO. 3.316), and *Penicillium expansum* (CGMCC NO. 3.7898).

2.2. Gene cloning and bioinformatics analysis

The specific primers (Table 1) for the *Anguinin* gene were crafted utilizing Primer Premier software (Version 5.0) and manufactured by Sangon Biotech Co., Ltd. (Shanghai, China). These primers were designed based on partial sequences from our research group's transcriptome database of the Japanese eel. To amplify the *Anguinin* gene's coding sequence (CDS), we used cDNA from the Japanese eel's spleen as a template with the primers Anguinin-CDS-F and Anguinin-CDS-R. For the 3′- and 5′- RACE cDNA templates from spleen tissue, we followed

Table 1
Primers used in the study.

Primer name	Primer sequences (5′-3′)
Anguinin-CDS-F	ATGAAGGGTTACGGAAACAA
Anguinin-CDS-R	CTAGAACGCACTGTCACTCAG
Anguinin-3′-F1	AAATCGCCTGTTCTCTGGTCCCG
Anguinin-3′-F2	CGTAAGTTTACCGGAAGCTGGACGC
Anguinin-5′-R1	GCGTCCAGCTTCCGGTAAACTTACG
Anguinin-5′-R2	CGGGACCAGAGAACAGGCGATTT
Anguinin-qPCR-F	GGAAACGTGGCATTCTCCTC
Anguinin-qPCR -R	CGGTAAACTTACGGCGCTTG
AjRPL8-qPCR-F	CCGTCAACCGGGTTTAGTTC
AjRPL8-qPCR-R	GATGTGCCGGAGTTTAGCAG
AjIL8-qPCR-F	CCTGCATGCTGTGAAAGGAG
AjIL8-qPCR-R	ACAGGGCCTTCCTTCCTCT
AjIL6-qPCR-F	CCGCTGACCTATCTGCTCAT
AjIL6-qPCR-R	TCCAGCTGGTCAGGCTTAAA
AjTNFα-qPCR-F	ACAGCCAAGTCTCATTCCGA
AjTNFα-qPCR-R	GTTTGCATCACTCTGGCACA

established methods [28]. The 5′- and 3′- untranslated regions (UTRs) of the *Anguinin* gene were amplified *via* nested PCR. In the initial PCR, we employed primers Anguinin-5′-R1 and Anguinin-3′-F1, followed by Anguinin-5′-R2 and Anguinin-3′-F2. Additionally, universal primers from the SMARTer® RACE 5′/3′ Kit were included in our protocol. The touch-down PCR protocol involved: an initial denaturation at 95 °C for 5 min; 30 cycles of 95 °C for 30 s, annealing at 72 °C (decreasing by 0.5 °C per cycle) for 30 s, and extension at 72 °C for 90 s; followed by a final extension at 72 °C for 5 min and a hold at 16 °C. The purified PCR products were then ligated into the pMD18-T vector (Takara, Japan) and transformed into *E. coli* DH5α competent cells. Positive clones were identified by colony PCR, and at least three independent clones for each fragment were sequenced by Sangon Biotech (Shanghai, China).

The physicochemical properties of amino acid sequences were predicted using the ExPASy platform (https://www.expasy.org/). The similarity analysis of amino acid and nucleotide sequences was performed using DNAMAN software (Version 8.0). Protein 3D structure predictions were conducted with I-TASSER (https://zhanggroup.org/I-TASSER/) and AlphaFold2 (https://github.com/deepmind/alphafold), with visualization accomplished using PyMOL software (Version 2.5.8).

2.3. Quantitative PCR (qPCR) analysis

Absolute qPCR was conducted to assess the tissue-specific distribution of the *Anguinin* gene in *A. japonica*. Additionally, to assess the tissue-specific expression profile of the *Anguinin* gene, relative qPCR was performed using *RPL8* as the internal reference. Tissues (intestine, liver, and spleen) were collected following infection with a sublethal dose of *E. tarda* (2.0×10^5 CFU/fish), a dosage selected in accordance with established Japanese eel infection models to induce a robust innate immune response while minimizing mortality and acute tissue damage [29,30]. Moreover, the expression of inflammation-associated genes (including *IL-6*, *IL-8*, and *TNF-α*) in the liver of Japanese eel challenged with *E. tarda* or treated with $Anguinin_{55–72}$ were analyzed by relative qPCR.

qPCR was conducted utilizing the CFX384 Real-Time PCR Detection System (Bio-Rad, USA), following the methods detailed in previous publications [28]. Relative qPCR data were analyzed applying the $2^{-\triangle\triangle Ct}$ method [31].

2.4. Peptide design and synthesis

The antimicrobial region of Anguinin was predicted using the $CAMP_{R4}$ database (http://www.camp.bicnirrh.res.in/). Based on this prediction and several key parameters for antimicrobial peptide design—including net positive charge, hydrophobicity, and α-helical propensity—an 18-residue fragment, $Anguinin_{55–72}$ (KFTGSWTRGAWGRAVVRR), was selected and chemically synthesized by GenScript (Nanjing, China) with a purity of 96.9%. The synthesized peptide was stored in lyophilized form at −20 °C until further use.

2.5. Circular dichroism (CD) spectroscopy

The secondary structure of $Anguinin_{55–72}$ was analyzed using a CD spectrometer (Jasco J-810, Japan). The peptide was dissolved in ultrapure water and 60 mM SDS at a final concentration of 0.1 mg/mL. Spectra were recorded between 190 and 260 nm using a 100-mm pathlength quartz cuvette with a scan speed of 100 nm/min.

2.6. Antimicrobial assay

A modified broth microdilution method [32] was employed to evaluate the antimicrobial activity of $Anguinin_{55–72}$. A concentration of about 10^6 CFU/mL was achieved by diluting bacteria in the logarithmic growth phase in Muller-Hinton broth (HKM, China), followed by incubation in 96-well flat-bottomed plates (NEST, China). They were then exposed to peptide concentrations ranging from 3 to 96 μM at their corresponding optimal temperature for 24 h. The minimum inhibitory concentration (MIC) was determined as the lowest peptide concentration that inhibited visible bacterial growth, and the minimum bactericidal concentration (MBC) was identified as the concentration that resulted in the death of over 99.99% of bacteria. The assay was conducted in triplicate at least three times.

2.7. The time killing kinetics

A Gram-positive *S. epidermidis* and a Gram-negative *A. baumannii* were chosen for the time-killing kinetic assay, following a method similar to previous reports [33]. In brief, the concentration of bacteria in the logarithmic growth phase was adjusted to about 10^6 CFU/mL using MH medium. $Anguinin_{55–72}$ at concentrations equivalent to 1 × MBC and 2 × MBC in a 1:1 ratio was then mixed with bacteria and incubated at 37 °C. At intervals of 0, 5, 10, 20, 30, 60, 120, 240, and 360 min, samples were collected and spread evenly on nutrient broth (NB) agar plates. These plates were cultured at 37 °C for 20–24 h to allow growth of surviving bacteria, which were subsequently counted. A control was also set up using medium without the peptide. Each experiment was conducted in triplicate, with three independent repetitions.

2.8. Scanning electron microscope (SEM) observation

SEM was used to evaluate the effect of $Anguinin_{55–72}$ on *S. epidermidis* and *A. baumannii*, following a previously described protocol [34]. Bacteria in the logarithmic growth phase were resuspended to a concentration of about 10^8 CFU/mL in 10 mM sodium phosphate buffer (NaPB), followed by incubation with $Anguinin_{55–72}$ (1 × MBC) for 20 min at 37 °C. Subsequently, the samples were stabilized with 2.5% glutaraldehyde solution overnight. After fixation, the samples underwent washing, resuspended in NaPB, and spread onto glass slides on ice. Ethanol was then employed for sample dehydration, and a critical point dryer (EM CPD300, Leica, Germany) was used for drying. Finally, the samples were coated with gold and analyzed using a SEM (Zeiss SUPRA 55, Germany).

2.9. Transmission electron microscope (TEM) observation

TEM analysis was conducted based on the established experimental protocol [35]. Briefly, *S. epidermidis* and *A. baumannii* were incubated with $Anguinin_{55–72}$ for 20 min, respectively. Following incubation, the bacterial cells were washed with NaPB and transferred onto an agar medium. Subsequently, the samples were stabilized with a 2.5% glutaraldehyde solution at 4 °C overnight. After fixation, the samples

underwent three cycles of washes with NaPB for 15 min each. They were further treated with a 1% osmium tetroxide solution for 1 h, to postfix, followed by dehydration and rinsing. The samples were then impregnated with epoxy resin for stabilization. Finally, the cell structures were visualized utilizing a TEM (HT-7800, Hitachi, Japan).

2.10. Assessment of outer membrane permeability

The *N*-phenyl-L-naphthylamine (NPN, Sigma, Germany) assay was used to assess the effect of Anguinin$_{55–72}$ on bacterial outer membrane permeability. During the logarithmic growth phase, *S. epidermidis* and *A. baumannii* cells were resuspended in HEPES buffer (pH 7.4, with 5 mM glucose) to achieve a concentration of about 10^8 CFU/mL. NPN was added to the bacterial suspensions to a final concentration of 10 μM. The mixtures were then transferred to a 96-well black flat-bottomed microtiter plate (NUNC, Roskilde, Denmark), and fluorescence was detected with a microplate reader at 350/420 nm until a stable baseline was established. Subsequently, Anguinin$_{55–72}$ with various concentrations (1.5 μM, 3 μM, 6 μM, 12 μM, 24 μM, 48 μM) were added to the wells, with Milli-Q water as a negative control and 1 μg/mL polymyxin B (PMB) as a positive control. Fluorescence intensity changes were monitored every 2 min, and each experiment was performed in triplicate, with three independent repetitions.

2.11. Inner membrane permeability assay

The effect of Anguinin$_{55–72}$ on bacterial inner membrane permeability was determined with the LIVE/DEAD BacLight™ staining kit (Thermo Fisher, USA), following the established method [36]. Briefly, *S. epidermidis* and *A. baumannii* in the exponential growth period were collected and washed three times in 10 mM NaPB (pH 7.4) to achieve a concentration of about 10^7 CFU/mL. The bacterial suspensions were subsequently treated with Anguinin$_{55–72}$ at a concentration of 1 × MBC for 15 min at 37 °C. After another three washes, SYTO 9 and propidium iodide (PI) were added for bacterial staining. The samples were then incubated for 15 min at 37 °C in the dark and analyzed using a confocal laser scanning microscopy (CLSM) (Zeiss LSM780, Germany).

2.12. Lipoteichoic acid and lipopolysaccharides inhibition assays

25 μL of Anguinin$_{55–72}$ at a final concentration equivalent to 1 × MIC was added to a 96-well flat-bottom plate. To this, 25 μL of lipoteichoic acid (LTA) from *S. aureus* (Sigma, USA) or lipopolysaccharides (LPS) from *E. coli* (Sigma, USA) was introduced, with the final concentration of each ranging from 8 to 64 mg/mL. The mixtures were incubated at room temperature for 20 min to reach equilibrium. Following this, 50 μL of *S. epidermidis* or *A. baumannii*, each at a concentration of about 10^6 CFU/mL, were introduced into the corresponding wells. They were then exposed to the Anguinin$_{55–72}$-LTA or Anguinin$_{55–72}$-LPS mixtures for 24 h at 37 °C. The optical density of each well was determined at 595 nm with a microplate reader (Tecan, Switzerland). Each experiment was conducted in triplicate and replicated at least three separate occasions.

2.13. Assessment of reactive oxygen species (ROS) production and ROS inhibition assay

The fluorescent probe 2′,7′-dichlorodihydrofluorescein diacetate (DCFH-DA), obtained from the Nanjing Jiancheng Bioengineering Institute, was used to measure ROS production by bacteria treated with Anguinin$_{55–72}$. The concentrations of *S. epidermidis* and *A. baumannii* were standardized to 1 × 10^8 CFU/mL in a mixture containing NaPB and 40% MHB. These bacterial suspensions were subsequently treated with different concentrations of Anguinin$_{55–72}$ (ranging from 1.5 μM to 48 μM) or polymyxin B (PMB) (1 μg/mL), and incubated for 30 min. After three rinses with PBS, the bacteria were treated with DCFH-DA (10 μM) for an additional 30 min. The levels of ROS were assessed by measuring fluorescence intensity with a microplate reader, using excitation and emission spectra of 488 nm and 533 nm, respectively. The experiment was conducted in triplicate and repeated three separate occasions.

To further investigate whether ROS generation directly contributes to the bactericidal activity of Anguinin$_{55–72}$, a ROS scavenging assay was performed using thiourea (Macklin, China) [37]. First, a specific verification experiment was conducted to evaluate the effect of the ROS scavenger. *S. epidermidis* and *A. baumannii* (1 × 10^8 CFU/mL) were assigned to four distinct groups: (i) control group (untreated bacteria), (ii) thiourea-only group (100 mM thiourea), (iii) peptide-only group (treated with Anguinin$_{55–72}$ at 1 × MBC), and (iv) co-treatment group (treated with 1 × MBC peptide and 100 mM thiourea). After co-incubation, the intracellular ROS levels were detected. Subsequently, a concentration-dependent bactericidal assay was performed. The bacteria were treated with various concentrations of Anguinin$_{55–72}$ (ranging from 1.5 to 48 μM) in the presence or absence of 100 mM thiourea. After co-incubation for 1 h, the bacterial suspensions were serially diluted and plated on nutrient agar plates to determine the colony-forming units. The survival rates were compared between the group treated with the peptide alone and the group co-treated with thiourea to evaluate the specific role of oxidative stress in the peptide's lethality. All experiments were independently repeated at least three times.

2.14. Biofilm inhibition assays

The effect of Anguinin$_{55–72}$ on biofilm formation was assessed using the method reported in a previous study [38]. In Brief, *S. epidermidis* and *A. baumannii* in the logarithmic growth phase were harvested and washed with NaPB. They were then diluted to a concentration of 1 × 10^8 CFU/mLin MH medium. In 96-well plates, these diluted bacteria were co-incubated with varying concentrations of Anguinin$_{55–72}$ (ranging from 0 to 48 μM) for 24 h. After incubation, the biofilms were stained with 0.1% crystal violet (CV, Sigma, Germany), and the staining was quantified by measuring the absorbance at 595 nm using a microplate reader. Each experiment was performed with six replicates and was independently conducted three times.

In the preformed biofilm experiments, *S. epidermidis* and *A. baumannii* at a concentration of about 10^6 CFU/mL were cultured at 37 °C for 24 h in a static condition to facilitate biofilm development. Afterwards, Mueller-Hinton (MH) medium containing Anguinin$_{55–72}$ and resazurin (0.1 mM), was added to the wells. The microplates were then cultured at 37 °C for an additional 24 h. The viability of the biofilm-associated cells was assessed using a modified resazurin test, as detailed in a previous study [39].

2.15. Sodium ion tolerance and thermal stability assay

To assess Na^+ tolerance, *S. epidermidis* and *A. baumannii* were collected during the logarithmic growth phase and adjusted to a concentration of around 10^6 CFU/mL. Subsequently, the diluted bacterial suspensions were co-incubated with Anguinin$_{55–72}$ (1 × MIC), along with varying concentrations of sodium chloride (NaCl) ranging from 20 to 160 mM in microtiter plate wells at 37 °C for 24 h. The experiment was conducted using a microplate reader to detect the absorbance at 595 nm. This experiment was performed in three replicates and independently repeated at least three separate occasions.

Similarly, the thermal stability of the bacteria was evaluated by mixing the prepared bacteria with heat-treated Anguinin$_{55–72}$ (100 °C for 10, 20 and 30 min), followed by incubation at 37 °C for 24 h. The viability of bacteria was assessed by measuring absorbance at 595 nm using a microplate reader. This assay was also conducted in triplicate and repeated at least three separate occasions.

2.16. Cytotoxicity assay of Anguinin$_{55–72}$ and in vivo anti-infective effect on E. tarda infected zebrafish

The cytotoxic effects of Anguinin$_{55–72}$ on HEK293T and ZF4 cells were assessed with the MTS assay, following a previously described method [38]. First, HEK293T and ZF4 were diluted to a density of around 10^5 cells/mL and cultured for 10 h at 37 °C and 28 °C, respectively, under a 5% CO_2 atmosphere. Subsequently, fresh medium containing various concentrations of Anguinin$_{55–72}$ (6, 12, 24, 48, and 96 μM) was added to replace the original culture medium, and the cells were incubated for an additional 24 h Each independent experiment included five replicates, and the entire assay was conducted three times independently.

Next, we examined the *in vivo* anti-infective properties of Anguinin$_{55–72}$ using an adult zebrafish model exposed to *E. tarda*. In brief, zebrafish were randomly assigned to four groups, each consisting of 20 fish. Bacteria in the logarithmic growth stage were harvested and rinsed three times using fish saline to achieve a final concentration of 1×10^8 CFU/mL. The zebrafish were injected intraperitoneally with the bacterial suspension at a volume of 8.8 μL per fish (resulting in an actual dose of approx. 1×10^6 CFU/fish, which was pre-determined as the minimum LD_{100} for this model). One hour after infection, they were further injected with Anguinin$_{55–72}$ (1 mg/mL), also at a volume of 8.8 μL per fish. The control group was injected with fish saline one hour after receiving an injection of *E. tarda*, with an approximate dose of 10^6 CFU per fish. The survival of each group of fish was closely monitored and recorded over a 72-h period. Survival data were plotted using GraphPad Prism version 9.0.0 (San Diego, CA, USA). The experiment was conducted three times independently.

2.17. Evaluation of the in vivo protective efficacy of Anguinin$_{55–72}$ on E. tarda infected Japanese eel

we explored the *in vivo* anti-infective properties of Anguinin$_{55–72}$ using a model of Japanese eel infected with *E. tarda*. The eels were randomly assigned to three groups, each containing 20 individuals. Bacteria in the logarithmic growth stage were rinsed three times with fish saline to prepare the infection model. The Japanese eel in each group were administered an intraperitoneal injection of the bacterial suspension, containing 2.2×10^8 CFU per eel (a dosage corresponding to the LD_{50}). One hour after infection, they were administered an injection of Anguinin$_{55–72}$ at a dosage of 40 μg per eel. The control group was injected with fish saline one hour after the *E. tarda* inoculation. Survival rates of eels in each group were tracked and recorded closely over a 72-h period, and the survival rates were plotted using GraphPad Prism software version 9.0.0.

At the last time point, we evaluated several health indices of the Japanese eel in each groups, including the disease activity index (DAI), liver index (liver weight/fish weight $\times 10^4$), and spleen index (spleen weight/fish weight $\times 10^4$). The features graded for the DAI include swimming ability, body surface bleeding condition, degree of liver enlargement and congestion, among others. The detailed scoring criteria are shown in Table 4. Subsequently, samples of the eel livers were weighed and treated with sterile PBS to form a homogeneous suspension. The resulting homogenates were then serially diluted, spread evenly on nutrient agar plates, and incubated at 37 °C for 24 h to facilitate colony-forming unit (CFU) counting. Additionally, the levels of pro-inflammatory factors (including *IL-6*, *IL-8*, and *TNF-α*) in the *E. tarda*-challenged Japanese eels treated with Anguinin$_{55–72}$ were analyzed using relative quantitative PCR, with *RPL8* serving as the control gene. The $2^{-\Delta\Delta Ct}$ method was used to conduct the expression pattern analysis [31]. Finally, histopathological examination was conducted on liver sections from each group of Japanese eels using HE staining to evaluate the pathological changes.

2.18. Statistical analysis

Statistical analyses were performed with GraphPad Prism version 9.0.0 and SPSS version 26.0. One-way ANOVA analysis followed by the Dunnett *post hoc* test for multiple comparisons or Student's *t*-test for pairwise comparisons was used to evaluate the data between groups. A *p*-value less than 0.05 was considered statistically significant.

3. Results

3.1. Sequence analysis of Anguinin and truncated peptide design

We successfully cloned the complete cDNA sequence of a new functional gene, designated as *Anguinin* (Genbank Accession NO. PP826360), using RACE PCR with reference to the Japanese eel (*A. japonica*) transcriptomic database previously established in our lab. The gene is composed of a 320 bp 5′ UTR, a 432 bp 3′ UTR, and a 300 bp open reading frame (ORF) (Fig. 1A). And the ORF of *Anguinin* encodes a 99-amino acid protein with high sequence similarity to two unidentified functional genes from *Anguilla anguilla* (Genbank Accession NO. XM 035405582.1) and *Anguilla rostrata* (Genbank Accession NO. XM 064322250.1). No significant protein sequence similarity was found with other known proteins. The three-dimensional structure showed that Anguinin contains α-helix, β-fold, and random coiling (Fig. 1B), and Anguinin was identified as a cationic protein with a computed molecular weight of 10.63 kDa and an estimated isoelectric point (pI) of 12.01 (Table 2). Bioinformatics analysis of Anguinin was conducted on Anguinin to identify potential AMPs. This analysis led to the discovery of a peptide comprising 18 amino acid residues, designated as Anguinin$_{55–72}$, with the sequence KFTGSWTRGAWGRAVVRR. As depicted in Fig. 1C, the predicted tertiary structure of Anguinin$_{55–72}$ suggests that it adopts a typical α-helical conformation. To verify the predicted α-helical structure, CD spectroscopy was performed. In aqueous solution, Anguinin$_{55–72}$ exhibited a typical random coil conformation with a strong negative minimum near 200 nm. In contrast, in the membrane-mimetic 60 mM SDS environment, the peptide displayed a characteristic α-helical spectrum, featuring two negative minima at 208 and 222 nm and a prominent positive maximum at approximately 195 nm (Fig. 1D). Furthermore, the physicochemical characteristics of Anguinin$_{55–72}$ classify it as a cationic amphiphilic peptide, with an estimated net charge of +5 and a hydrophobicity percentage of 26.7% (Table 2). Multi-model prediction using the $CAMP_{R4}$ platform confirmed Anguinin$_{55–72}$ as an AMP, with high probability scores across 0.95 (Random Forest), 0.84 (Support Vector Machine), and 0.83 (Artificial Neural Network) architectures.

3.2. Anguinin gene expression patterns

The expression patterns of *Anguinin* in various tissues of Japanese eel were analyzed (Fig. 2A). The qPCR results showed that *Anguinin* exhibited the highest abundance in muscle, followed by relatively lower levels in skin and brain. Furthermore, after *E. tarda* infection in *A. japonica*, *Anguinin* was significantly upregulated in intestine at 24 h post-infection (Fig. 2B), in liver at 12 and 24 h post-infection (Fig. 2C), and in the spleen at 24 h post-infection and significantly downregulated at 48 h post-infection in the spleen (Fig. 2D).

3.3. Antimicrobial activity assessment of Anguinin$_{55–72}$

Antibacterial assays showed that Anguinin$_{55–72}$ had a broad antimicrobial spectrum, as summarized in Table 3. Anguinin$_{55–72}$ significantly inhibited multiple Gram-positive bacteria, including *E. faecium*, *S. epidermidis*, and L. *monocytogenes*, in addition to Gram-negative bacteria such as *A. baumannii*, *P. fluorescens*, *V. harveyi*, *V. alginolyticus* and *V. parahaemolyticus*, with MIC and MBC values not exceeding 24 μM. Furthermore, Anguinin$_{55–72}$ exhibited antifungal activity against the

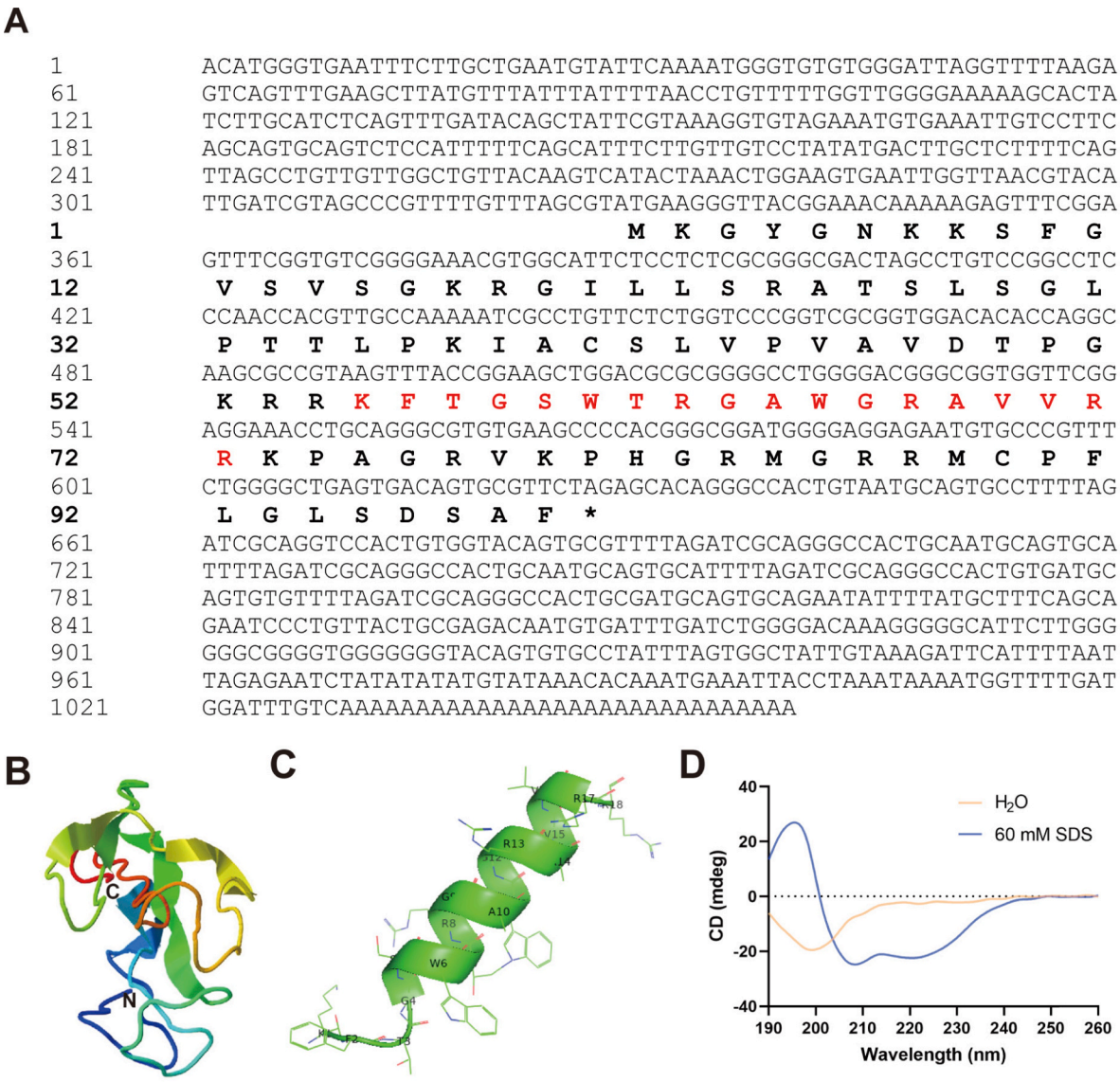

Fig. 1. Full-length cDNA sequence, amino acid sequence and three-dimensional structure of Anguinin and three-dimensional structure of Anguinin$_{55–72}$. (A) The complete cDNA sequences of *Anguinin* and the corresponding deduced amino acid sequences. (B) A computationally predicted three-dimensional structure of Anguinin generated using the I-TASSER program. (C) The predicted three-dimensional structure of Anguinin$_{55–72}$ by AlphaFold. (D) Secondary structure characterization of Anguinin$_{55–72}$ by Circular Dichroism (CD) spectroscopy.

Table 2
Sequence information and physicochemical properties of Anguinin and Anguinin$_{55–72}$.

Physicochemical parameters	Anguinin	Anguinin$_{55–72}$
Number of amino acids	99	18
Molecular MW (kDa)	10.63	2.09
Theoretical PI	12.01	12.8
Formula	$C_{470}H_{779}N_{149}O_{122}S_5$	$C_{94}H_{147}N_{33}O_{22}$
Total number of atoms	1525	296
Grand average of hydropathicity	−0.277	−0.683
Total net charge	+19	+5
Hydrophobic residue%	–	26.7%
Hydrophobic moment	–	0.089

germination of conidia of several filamentous fungi, including *F. solani*, *A. niger*, and *P. expansum*, with MIC values varying between 1.5 and 12 μM.

3.4. Bactericidal kinetics of Anguinin$_{55–72}$

The bactericidal efficacy of Anguinin$_{55–72}$ was assessed through kinetic studies. When incubated with *S. epidermidis*, Anguinin$_{55–72}$ at 1 × MBC resulted in a 99% reduction of bacteria within 120 min, and Anguinin$_{55–72}$ at 2 × MBC killed 99% bacteria within 60 min (Fig. 3A). Comparatively, a markedly slower bactericidal rate was observed against *A. baumannii*, which required double the exposure time (240 min at 1 × MBC and 120 min at 2 × MBC) to reach the same 99% killing efficiency (Fig. 3B).

3.5. Bacterial morphology changes after Anguinin$_{55–72}$ treatment

SEM and TEM were utilized to examine the morphological changes of *S. epidermidis* and *A. baumannii* following exposure to Anguinin$_{55–72}$. The findings indicated that after treatment with Anguinin$_{55–72}$, the bacterial cell membrane integrity was disrupted, resulting in the release of intracellular material (Fig. 3C and D). In contrast, the surfaces of untreated bacterial cells remained intact and smooth.

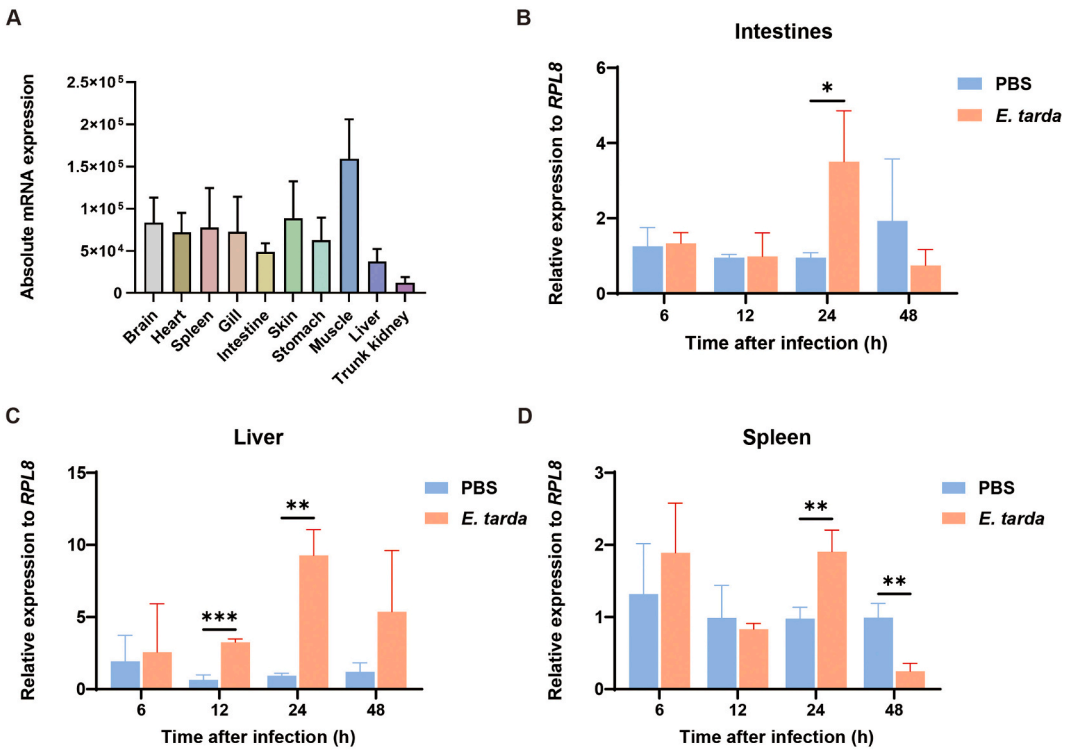

Fig. 2. Gene expression analysis of *Anguinin* in *A. japonica*. (A) Tissue-specific expression of the *Anguinin* gene in Japanese eel ($n = 5$). The expression pattern of *Anguinin* in the intestines (B), liver (C), and spleen (D) following *E. tarda* challenge ($n = 3$). Data are pexpressed as mean ± standard error of the mean ($n = 3$). Statistical significance was determined using Student's *t*-test. Statistical significance is denoted by asterisks as $^{*}p < 0.05$, $^{**}p < 0.01$, $^{***}p < 0.001$.

Table 3
Antimicrobial activity of Anguinin$_{55–72}$.

Microorganism	CGMCC NO.[a]	MIC[b] (μM)	MBC[c]/MFC[d] (μM)
Gram-positive bacteria			
Listeria monocytogenes	1.10753	3–6	12–24
Enterococcus faecium	1.131	6–12	12–24
Staphylococcus epidermidis	1.4260	12–24	12–24
Staphylococcu saureus	1.2465	24–48	24–48
Gram-negative bacteria			
Acinetobacter baumannii	1.6769	3–6	3–6
Pseudomonas fluorescens	1.3202	3–6	3–6
Pseudomonas putida	1.1836	3–6	3–6
Escherichia coli	1.2389	6–12	6–12
Pseudomonas aeruginosa	1.2421	12–24	12–24
Vibrio harveyi	1.1593	0–1.5	0–1.5
Vibrio alginolyticus	1.1833	3–6	3–6
Vibrio parahaemolyticus	1.1615	3–6	6–12
Vibrio fluvialis	1.1609	6–12	12–24
Edwardsiella tarda	1.1872	>48	>48
Fungi			
Crytococcus neoformans	2.1563	1.5–3	1.5–3
Fusarium solani	3.5840	1.5–3	1.5–3
Aspergillus niger	3.316	6–12	6–12
Penicillium expansum	3.7898	6–12	6–12

[a] China General Microbiological Culture Collection Center.
[b] The values of MIC were expressed as the interval A-B. A was the highest concentration tested with visible microbial growth, whereas B was determined as the lowest concentration without visible microbial growth.
[c] The values of MBC presented are those wherein the peptide concentration killed 99.99% of the bacteria.
[d] The values of MFC presented are those wherein the peptide concentration killed 99.99% of the fungi.

Table 4
Disease activity index score rules.

Features graded	Score	Description
Swimming movement	0	Normal
	1	Slightly slow
	2	Slow
Body surface bleeding	0	None
	1	1–2 bleeding sites
	2	3–5 bleeding sites
	3	More than 5 bleeding sites
Severity of anal inflammation	0	Normal
	1	Slightly
	2	Medium
	3	Serious
Intestinal fluid retention	0	Normal
	1	Slightly
	2	Medium
	3	Serious
Hepatomegaly congestion degree	0	Normal
	1	Slightly
	2	Medium
	3	Serious
Splenomegaly and hemorrhagic spots	0	Normal
	1	Slightly
	2	Medium
	3	Serious

3.6. Anguinin$_{55–72}$ treatment increases bacterial outer and inner membranes permeability

Bacterial outer membranes are enrich with anionic polysaccharides that block the entry of cationic peptides into the inner membrane [40]. In this study, we evaluated the effect of Anguinin$_{55–72}$ on the outer membrane integrity of *S. epidermidis* and *A. baumannii* using the NPN probe. This probe can penetrate the damaged outer membranes and exhibits enhanced fluorescence upon interaction with lipophilic lipids.

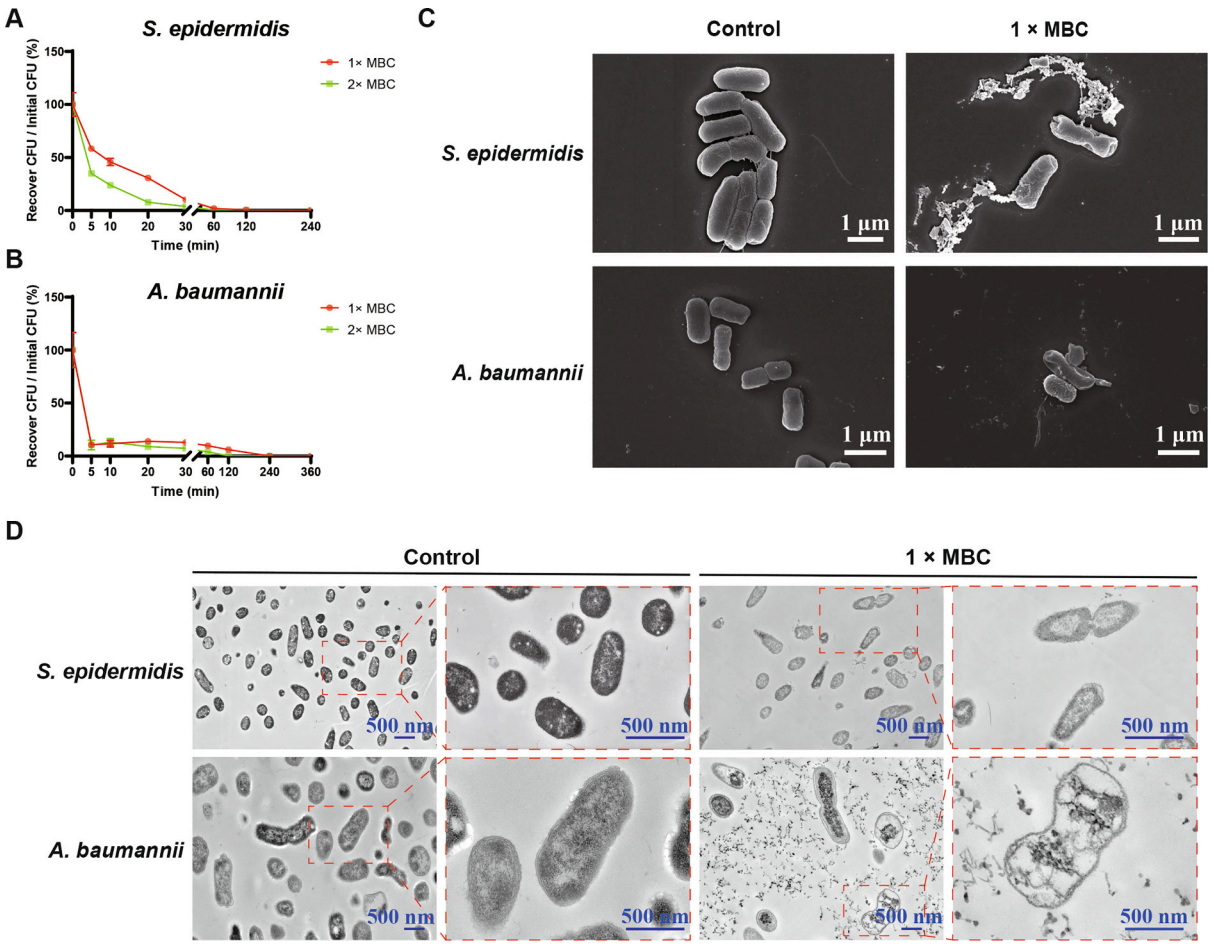

Fig. 3. Bactericidal effects of Anguinin$_{55–72}$ against bacteria. Time-dependent bactericidal activity of Anguinin$_{55–72}$ against *S. epidermidis* (A) and *A. baumannii* (B). (C) Surface morphological alterations of bacteria upon exposure to Anguinin$_{55–72}$ as visualized by SEM. (D) Internal structural alterations of bacteria iupon exposure to Anguinin$_{55–72}$ as visualized by TEM. MBC, minimum bactericidal concentration.

As illustrated in Fig. 4A and B, the fluorescence intensity of NPN escalated in tandem with increasing concentrations of Anguinin$_{55–72}$, indicating that increased outer membrane permeability was associated with membrane damage.

In addition, the permeability of the inner membrane in *S. epidermidis* and *A. baumannii* following Anguinin$_{55–72}$ treatment was assessed through SYTO 9 and PI fluorescence staining. When bacteria are incubated with SYTO 9 and PI, SYTO 9 stains all bacteria regardless of their membrane integrity, while PI staining is specific to bacteria with damaged membranes. The findings revealed that, in contrast to the untreated control which exhibited almost uniform green fluorescence, the bacteria treated with Anguinin$_{55–72}$ displayed a marked increase in red fluorescence, indicating that the bacterial membrane was damaged (Fig. 4C and D).

3.7. Effect of bacterial membrane components on the antibacterial efficacy of Anguinin$_{55–72}$

A common mechanism of AMPs is to bind to surface components and disrupt bacterial membranes, with LTA and LPS being the predominant components in Gram-positive and Gram-negative bacterial membrane, accordingly. Our study revealed that LPS, but not LTA, mitigated the bactericidal activity of Anguinin$_{55–72}$ in a concentration-dependent manner. As depicted in Fig. 5A, the antibacterial efficacy of Anguinin$_{55–72}$ remained unaffected by the presence of exogenous LTA in the range of 8 to 64 μg/mL. In contrast, the addition of LPS at concentrations ranging from 16 to 64 μg/mL significantly affected the antibacterial effectiveness of Anguinin$_{55–72}$ against *A. baumannii*, as shown in Fig. 5B. The inhibitory action of Anguinin$_{55–72}$ against *A. baumannii* was observed to decrease with the increase of LPS concentrations. This suggests that Anguinin$_{55–72}$ may target Gram-negative bacteria by interacting with LPS, rather than targeting Gram-positive bacteria through binding to LTA.

3.8. Increase in bacterial endogenous ROS after Anguinin$_{55–72}$ treatment

AMPs are known to amplify bacterial membrane damage by triggering the production of ROS [41]. We examined the ROS concentrations in *S. epidermidis* or *A. baumannii* following treatment with Anguinin$_{55–72}$. The results, presented in Fig. 5C and F, demonstrated that Anguinin$_{55–72}$ stimulated the intracellular generation of ROS in both bacterial strains, with the level of accumulation correlating positively with the concentration of Anguinin$_{55–72}$ applied.

3.9. Mechanistic role of ROS in the lethality of Anguinin$_{55–72}$

To evaluate the contribution of oxidative stress to the bactericidal action of Anguinin$_{55–72}$, a rescue assay was performed using the ROS scavenger thiourea. We first confirmed that thiourea (100 mM) effectively neutralized the Anguinin$_{55–72}$-induced intracellular ROS in both *S. epidermidis* and *A. baumannii*, as evidenced by the significant reduction in DCFH-DA fluorescence (Fig. 5D and G). Following this verification, we examined the impact of ROS scavenging on bacterial survival across a range of peptide concentrations. At relatively low

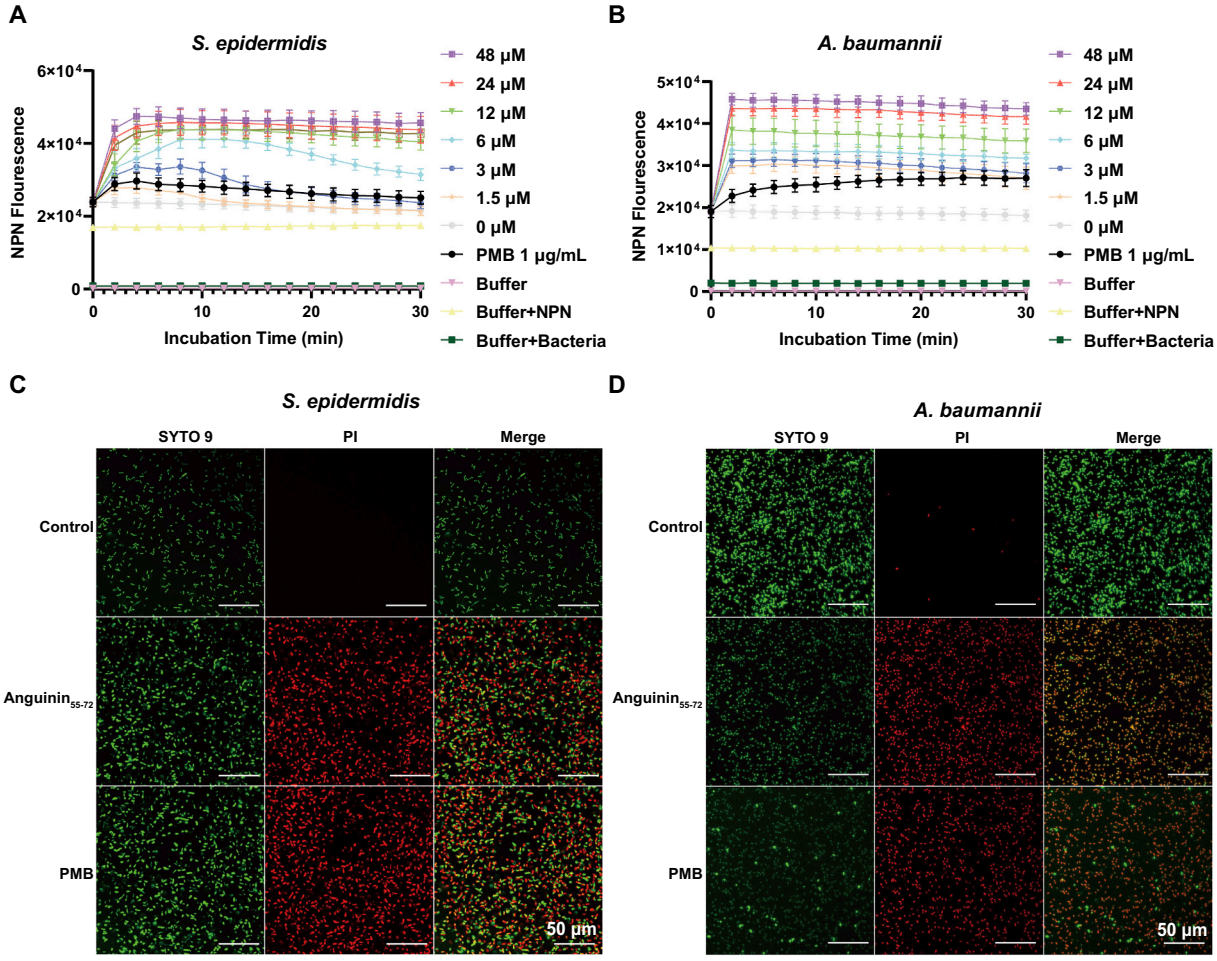

Fig. 4. Disruption of bacterial membrane integrity by Anguinin$_{55–72}$. Assessment of outer membrane permeability in *S. epidermidis* (A) and *A. baumannii* (B) following Anguinin$_{55–72}$ treatment was captured at excitation wavelengths of 350 nm and emission wavelengths of 420 nm. Impact of Anguinin$_{55–72}$ on the inner membrane permeability of *S. epidermidis* (C) and *A. baumannii* (D), visualized by CLSM following SYTO 9 and PI staining. In both inner and outer membrane permeability assays, PMB served as a positive control for membrane disruption. Scale bar: 50 nm.

concentrations of Anguinin$_{55–72}$, no significant difference in bacterial viability was observed between the groups treated with the peptide alone and those co-treated with thiourea. However, the protective effect of thiourea became prominent as the peptide concentration increased. Specifically, for *S. epidermidis*, a significant recovery in bacterial counts was observed in the thiourea-supplemented group when the peptide concentration reached 12 μM or higher (Fig. 5E). Similarly, for *A. baumannii*, the addition of thiourea significantly mitigated the lethal effect of Anguinin$_{55–72}$ at concentrations above 24 μM, resulting in a markedly higher number of surviving colonies compared to the peptide-only group (Fig. 5H). These results suggest that while ROS production might be limited at low peptide dosages, it becomes a crucial lethal factor at higher concentrations, significantly accelerating bacterial death.

3.10. Anti-biofilm effectiveness of Anguinin$_{55–72}$

Bacterial infections often lead to the development of biofilm structures, which greatly increase the difficulty of combating antibiotic resistance [39]. Biofilms can increase bacterial resistance to antibiotics by 10–1000-fold [42]. In light of this, our study evaluated the effect of various concentrations of Anguinin$_{55–72}$ (1.5 μM–48 μM) on the biofilm-formation capabilities of *S. epidermidis* and *A. baumannii*. The findings indicated that Anguinin$_{55–72}$ reduced biofilm formation of *A. baumannii* in a dose-dependent manner, while biofilm formation in *S. epidermidis* was only affected at 48 μM (Fig. 6A and B). Furthermore, the metabolic function of preformed biofilms of *S. epidermidis* and *A. baumannii* were assessed using the redox indicator resazurin following exposure to Anguinin$_{55–72}$. The results demonstrated that Anguinin$_{55–72}$ could suppress the respiration of both bacterial strains in the preformed biofilms in a concentration-dependent manner (Fig. 6C and D). These findings suggest that Anguinin$_{55–72}$ possesses anti-bacterial biofilm activity.

3.11. Stability evaluation of Anguinin$_{55–72}$

The stability assessment of Anguinin$_{55–72}$ encompassed evaluation of its antimicrobial efficacy under various conditions. Fig. 7A and B illustrate the impact of varying sodium ion concentrations on its activity. The findings showed that Anguinin$_{55–72}$ was unable to completely suppress the growth of *S. epidermidis* and *A. baumannii* at a sodium ion concentration of 40 mM and 20 mM, respectively. In addition, the bactericidal potency of Anguinin$_{55–72}$ against both *S. epidermidis* and *A. baumannii* was unaffected when subjected to heat treatment at 100 °C for 10 to 30 min (Fig. 7C and D). Collectively, these results indicated that Anguinin$_{55–72}$ maintained considerable stability under elevated temperature conditions but is sensitive to sodium ion.

3.12. Anguinin$_{55–72}$ was non-cytotoxic and improved zebrafish survival after *E. tarda* challenge

To assess the cytotoxicity of Anguinin$_{55–72}$, we utilized two cell lines: HEK293T and ZF4. The findings, as presented in Fig. 8A and B,

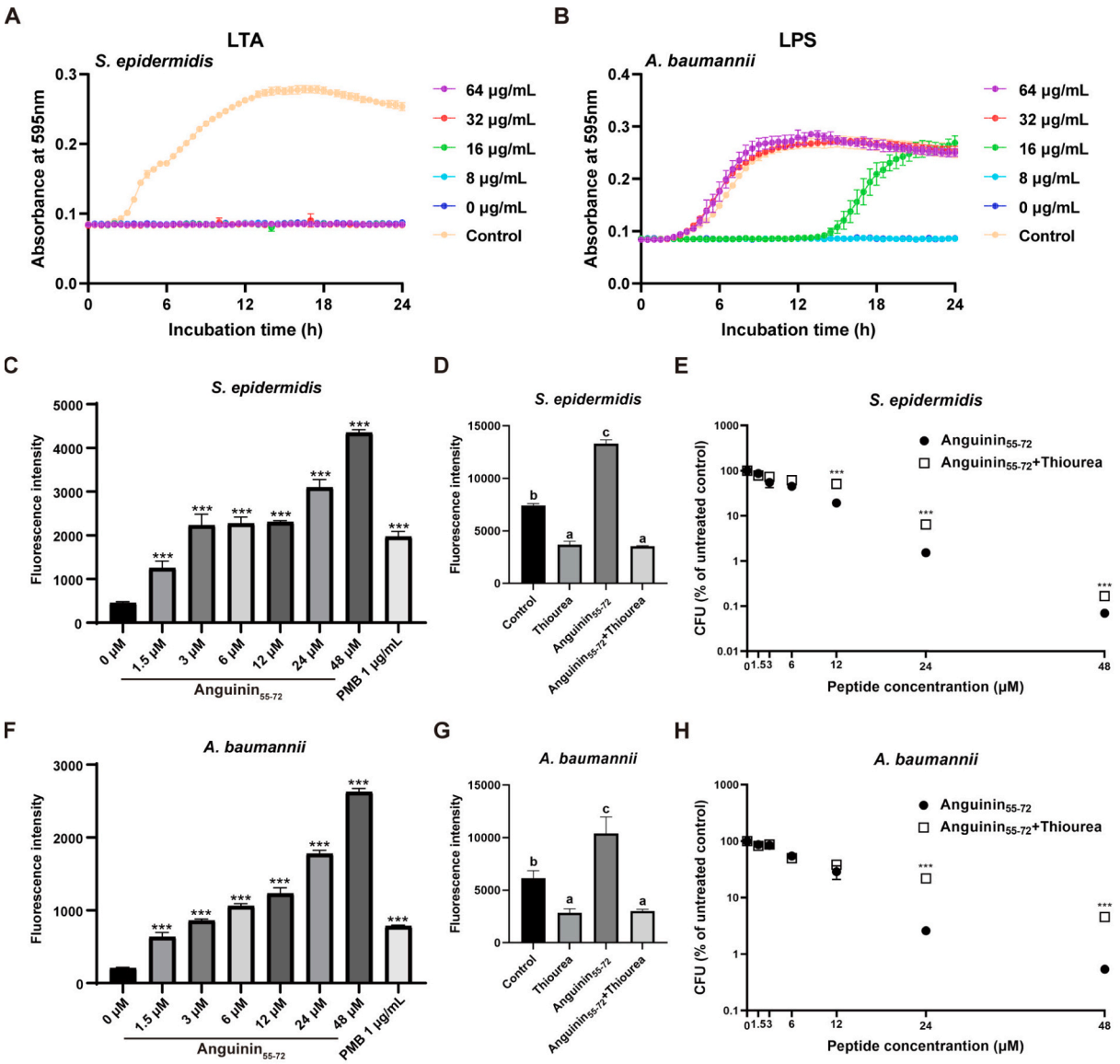

Fig. 5. Interaction of Anguinin$_{55–72}$ with bacterial membrane components and the mechanistic role of ROS in its bactericidal activity. The influence of exogenous LTA (A) and LPS (B) on the antibacterial activity of Anguinin$_{55–72}$ was evaluated by monitoring the growth curve of *S. epidermidis* and *A. baumannii*. Variations in intracellular ROS levels in *S. epidermidis* (C) and *A. baumannii* (F) following treatment with Anguinin$_{55–72}$, inferred from the fluorescence emitted upon DCFH-DA oxidation. Validation of ROS scavenging efficiency in *S. epidermidis* (D) and *A. baumannii* (G) using four experimental groups: control, thiourea only, peptide only, and co-treatment with thiourea and peptide. To validate the contribution of ROS to lethality, the survival rates of *S. epidermidis* (E) and *A. baumannii* (H) were measured after 1 h of treatment with Anguinin$_{55–72}$ in the presence or absence of 100 mM thiourea. LTA, lipoteichoic acid; LPS, lipopolysaccharides. Data are expressed as mean ± standard error of the mean ($n = 3$). Statistical significance was determined using one-way ANOVA followed by the Dunnett *post hoc* test (for C, and F) or the Tukey's *post hoc* test (for D and G), or Student's *t*-test (for E and H). Different lowercase letters indicate significant differences ($p < 0.05$) among groups. ***$p < 0.001$.

demonstrated that Anguinin$_{55–72}$ exhibited no cytotoxic effect toward either mammalian or zebrafish cells. Subsequently, we examined the effect of Anguinin$_{55–72}$ on *E. tarda* infected zebrafish. The data revealed that all zebrafish in the untreated group died within 42 h, while 25% of zebrafish in the Anguinin$_{55–72}$-treated group survived beyond 42 h, with 20% still alive at 72 h. The results indicated that Anguinin$_{55–72}$ considerably improved the survival rate of zebrafish ($p = 0.0411$) (Fig. 8C).

3.13. *Efficacy of Anguinin$_{55–72}$ treatment in a Japanese eel model of E. tarda infection*

We established a Japanese eel infection model to assess the antimicrobial and immunoregulatory effects of Anguinin$_{55–72}$ *in vivo*. *E. tarda* was administered intraperitoneally to the eels, followed by the treatment with Anguinin$_{55–72}$ one hour post-infection. After 72 h, the survival proportions of the Anguinin$_{55–72}$-treated and control groups were 80% and 50%, accordingly, with statistically significant differences ($p = 0.0496$) (Fig. 9A). Moreover, treatment with Anguinin$_{55–72}$ significantly decreased the disease activity index (mean from 9.2 to 3.0) (Fig. 9B), liver index (mean from 141.5 to 117.2) (Fig. 9C), spleen index (mean from 11.6 to 9.6) (Fig. 9D), and bacterial load in the liver (about 91.8%) (Fig. 9E). Subsequently, the mRNA levels of pro-inflammatory cytokines in the liver were further analyzed, and the results showed that inflammation-associated genes, including *IL8*, *IL6*, and *TNFα*, were significantly downregulated in Anguinin$_{55–72}$-treated Japanese eels (Fig. 9F). Finally, histopathological examination of liver tissue sections using HE staining revealed that the control group exhibited deformed

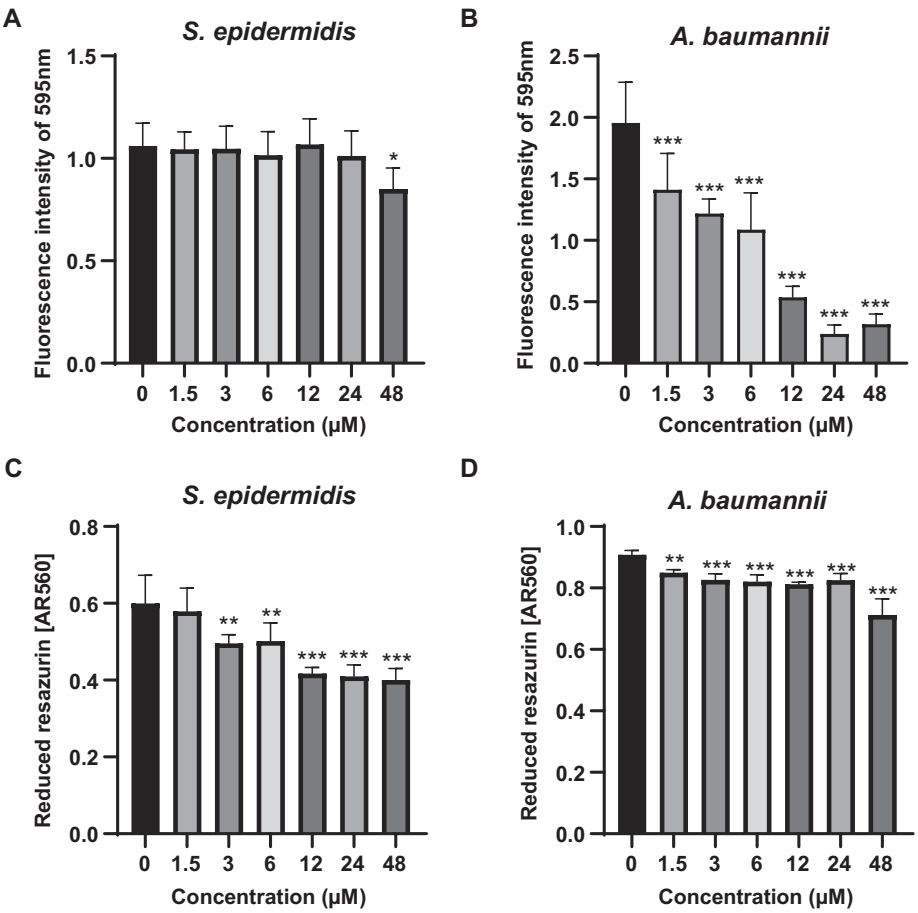

Fig. 6. Inhibition of *S. epidermidis* and *A. baumannii* biofilm by Anguinin$_{55–72}$. Quantitative assessment of the effect of various concentrations of Anguinin$_{55–72}$ on *S. epidermidis* (A) and *A. baumannii* (B) biofilm formation, as determined by crystal violet (CV) staining and absorbance measurement at 595 nm. Data are presented as mean ± standard error of the mean from six independent biological replicates. Statistical analysis was conducted using one-way ANOVA followed by the Dunnett *post hoc* test. *$p < 0.05$, ***$p < 0.001$. Inhibition of preformed *S. epidermidis* (C) and *A. baumannii* (D) biofilms by Anguinin$_{55–72}$, assessed by monitoring the reduction of resazurin to resorufin at 560 nm and the quantification of remaining oxidized resazurin at 620 nm. The corrected absorbance at 560 nm (AR560) was calculated using the formula: $AR560 = A_{560} - (A_{620} \times R_O)$ and $R_O = AO_{560}/AO_{620}$, where A_{560} and A_{620} represent the sample absorbance values, while AO_{560} and AO_{620} are the absorbance values of MH medium containing 0.1 mM resazurin. Data are presented as mean ± standard error of the mean ($n = 6$). Statistical analysis was conducted using one-way ANOVA followed by the Dunnett *post hoc* test. Significant difference between the control group and Anguinin$_{55–72}$ treatment group was indicated by asterisks as **$p < 0.01$, ***$p < 0.001$. (For interpretation of the references to colour in this figure legend, the reader is referred to the web version of this article.)

hepatocyte nuclei, nuclear hypertrophy, and cytoplasmic vacuolation, whereas the Anguinin$_{55–72}$ treated group showed substantial restoration of liver cell integrity (Fig. 9G).

4. Discussion

Bacterial pathogens are responsible for a wide range of diseases in the aquaculture industry, accounting for about 34% of all reported cases [43]. Particularly among eel diseases, bacterial infections are considered to be the most serious, with rapid onset and often leading to losses of up to 90% in farmed eels [44]. Among these pathogens, *E. tarda* stands out as a major threatening bacteria to eels, resulting in systemic infections and significant mortality [45]. Infected fish display symptoms including enlarged livers, hemorrhagic ascites, as well as bleeding and congestion on the skin and near the fin bases [46]. In aquaculture, antibiotics are commonly used to treat bacterial diseases in fish. However, the increase in the number of antibiotic-resistant strains has led to the regulation and restriction of antibiotic use in many countries globally [47]. Therefore, there is an urgent need to develop safer and more effective antimicrobial agents to control pathogens in aquaculture. Antimicrobial peptides (AMPs) are considered by scientists to be “natural antibiotics”, possessing broad-spectrum antimicrobial activity as well as multiple biological functions, including immune regulation [48]. The catadromous migratory fish, the eel, possesses a suite of unique physiological characteristics that enable it to survive in both the complex environments of rivers and the ocean throughout its life, thereby exposing it to a variety of pathogenic microorganisms. Therefore, the extraction of novel and effective antimicrobial peptides from this species holds great potential. In this study, we identified a new functional gene, *Anguinin*, in the transcriptomic database of the Japanese eels *A. japonica* challenged with *E. tarda*, which was significantly upregulated in tissues following bacterial stimulation. Through bioinformatics examination and experimental confirmation, we successfully characterized a novel AMP derived from Anguinin, designated as Anguinin$_{55–72}$. We investigated the physicochemical characteristics and *in vitro* antimicrobial effectiveness of Anguinin$_{55–72}$ and demonstrated its therapeutic efficacy against *E. tarda* infection *in vivo*, providing a theoretical basis and new insights for its future application in aquaculture.

In fish, despite the evolution of adaptive immunity, its underdeveloped nature means that fish mainly depend on their robust innate immune system to combat pathogens [49]. The principal immune organs implicated encompass the intestine, liver, spleen, and so on. [50]. In our research, upon invasion by *E. tarda*, the levels of *Anguinin* in the intestine, liver, and spleen at specific time points were significantly elevated. These results suggest that *Anguinin* could be essential for the immune defense of the Japanese eel. At present, the prevailing understanding is

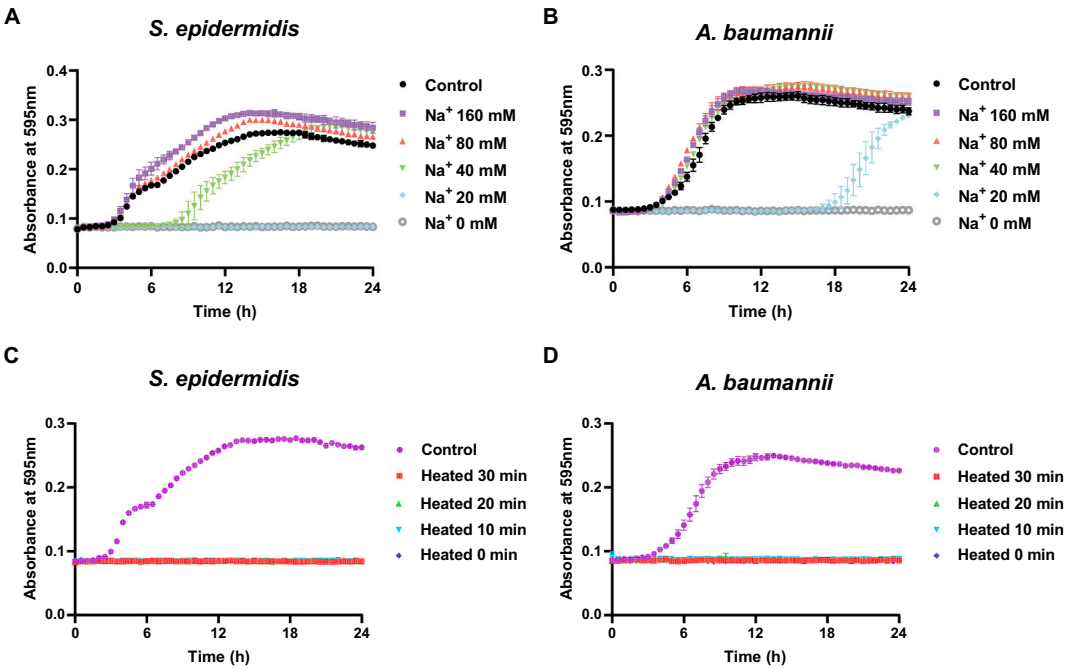

Fig. 7. Stability assessment of Anguinin$_{55–72}$. Variation in the antimicrobial activity of Anguinin$_{55–72}$ against *S. epidermidis* (A) and *A. baumannii* (B) at varying sodium ion concentrations. Impact of heat treatment at 100 °C on the antimicrobial activity of Anguinin$_{55–72}$ against *S. epidermidis* (C) and *A. baumannii* (D). The results were assessed by monitoring the OD600 values during bacterial growth ($n = 3$).

that the antimicrobial efficacy of AMPs is primarily determined by their hydrophobicity and net charge [51,52]. Anguinin$_{55–72}$, with a high positive charge (+5) and relatively low hydrophobicity (26.7%), exhibited potent antimicrobial activity against bacteria and fungi. Like other cationic AMPs, the positive charge of Anguinin$_{55–72}$ may facilitate its attachment to the anionic microbial surface *via* electrostatic interactions [51]. This interaction was further supported by our CD spectroscopy data, which demonstrated that Anguinin$_{55–72}$ underwent a dramatic conformational transition from a random coil in aqueous solution to a stable α-helical structure in membrane-mimetic SDS micelles. The characteristic peaks at 195, 208, and 222 nm confirmed its high helical propensity upon membrane binding. Simultaneously, our results from SEM and TEM also demonstrated that Anguinin$_{55–72}$ can induce bacterial death by disrupting the bacterial cell membrane. Further staining with SYTO9, PI, and NPN confirmed that Anguinin$_{55–72}$ can increase the permeability of both the inner and outer bacterial membranes, leading to the release of intracellular contents. This mechanism of action may be associated with the α-helical structure of Anguinin$_{55–72}$, similar to previously reported AMP [53].

Additionally, the effects of membrane components LTA and LPS on Anguinin$_{55–72}$'s antimicrobial activity revealed that LPS reduced its inhibitory effect against *A. baumannii*, while LTA did not affect its activity against *S. epidermidis* at the concentrations tested. This suggests that the bactericidal mechanism of Anguinin$_{55–72}$ against Gram-negative bacteria involves binding to LPS in the bacterial cell wall. When the peptide concentration reaches a certain level, it exerts its bactericidal effect by dissolving the bacterial cell membrane. This mechanism is similar to that of many cationic antimicrobial peptides, such as Epinecidin-1 [54]. However, it did not interact with LTA of Gram-positive bacterial membranes and may bind to other surface components (*e.g.*, peptidoglycan) of Gram-positive bacteria, a mechanism that warrants further investigation.

Moreover, we observed that Anguinin$_{55–72}$ induced an increase in bacterial ROS levels in a dose-dependent manner. ROS are produced through the electron transport chain during aerobic respiration and are essential for maintaining normal bacterial physiological activities [55]. However, excessive ROS accumulation during AMP treatment can cause oxidative stress, resulting in oxidative damage and impairing bacterial viability [56]. And our ROS scavenging experiments provide a more nuanced understanding of Anguinin$_{55–72}$'s mode of action. The observation that thiourea only offered protection at higher peptide concentrations (12 μM for *S. epidermidis* and 24 μM for *A. baumannii*) suggests a threshold effect for ROS-mediated lethality. At low concentrations, the antimicrobial activity of Anguinin$_{55–72}$ may primarily rely on initial membrane perturbations that do not immediately trigger a massive oxidative burst. However, as the peptide concentration increases, the intensified membrane disruption or deeper penetration into the cytoplasm likely triggers a robust and rapid accumulation of ROS, which then acts as a primary lethal driver to achieve complete bactericidal effects. This dual-mechanism—initial membrane destabilization followed by a concentration-dependent oxidative burst—ensures the high potency of Anguinin$_{55–72}$ against a broad spectrum of pathogens.

Furthermore, in experiments assessing the inhibitory and eradicative effects of Anguinin$_{55–72}$ on bacterial biofilms, we found that it was more effective at inhibiting Gram-negative bacteria biofilms than Gram-positive bacteria biofims, which may be related to its rapid bactericidal activity. Anguinin$_{55–72}$ can kill a large proportion of planktonic *A. baumannii* within a short period of time (approximately 90% killed within 5 min), thereby reducing bacterial adhesion and subsequent biofilm formation. Interestingly, Anguinin$_{55–72}$ achieved a 99% bactericidal rate against Gram-positive bacteria (*e.g.*, *S. epidermidis*) more rapidly than against Gram-negative bacteria (*e.g.*, *A. baumannii*). This difference is likely attributed to the distinct cell wall architectures of these two groups. Gram-negative bacteria possess an asymmetrical outer membrane (OM) rich in LPS, which acts as a sophisticated molecular sieve and a robust physical barrier, significantly restricting the penetration of amphipathic peptides to the inner membrane [57]. In contrast, Gram-positive bacteria lack this outer membrane barrier; their cell wall consists of a thick but porous peptidoglycan layer interspersed with LTA, which may allow cationic peptides to diffuse more readily and reach their target membrane sites [40]. Thus, the additional hurdle posed by the Gram-negative outer membrane likely accounts for the slightly delayed bactericidal kinetics observed in *A. baumannii*. Additionally, Anguinin$_{55–72}$ exhibited relatively weak efficacy in eradicating biofilms

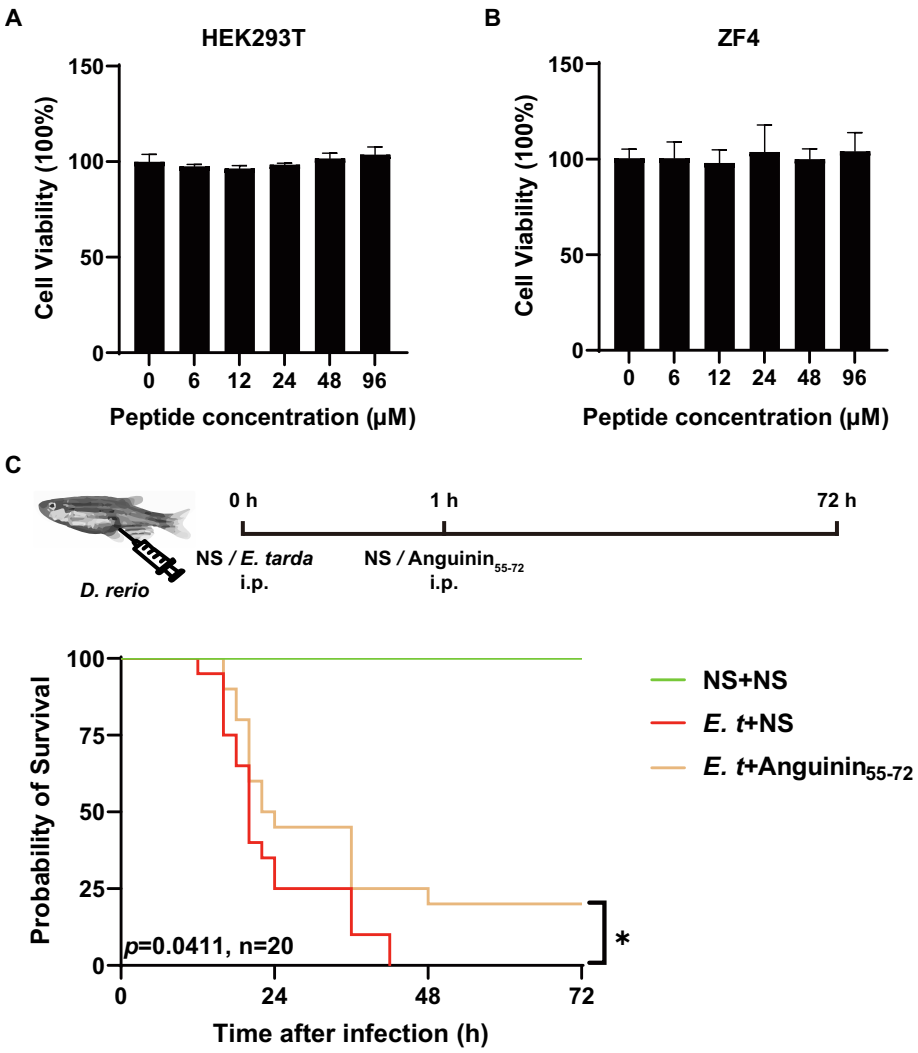

Fig. 8. Cytotoxicity and survival impact of Anguinin$_{55–72}$ post *E. tarda* Challenge in Zebrafish. Assessment of the cytotoxic effects of Anguinin$_{55–72}$ on ZF4 cells (A), and HEK293T cells (B) using the MTS-PMS assay. Bars indicate the mean ± standard error of the mean ($n = 5$). Experimental design for *E. tarda* infection in zebrafish and analysis of the survival rate using the Kaplan-Meier log-rank test ($n = 20$) (C).

of both types of bacteria, which may be due to the established thickness of the biofilm that restricts the penetration of Anguinin$_{55–72}$, preventing it from reaching effective bactericidal concentrations within the biofilm [58].

To further evaluate the potential application of Anguinin$_{55–72}$, we assessed its tolerance to sodium ions, thermal stability, and cytotoxicity. The results showed that Anguinin$_{55–72}$ exhibited tolerance to sodium ions in the range of 20 mM to 40 mM. This observed salt sensitivity potentially reflects an evolutionary adaptation to the freshwater-dominant life cycle of the Japanese eel. During its residence in rivers and lakes, the low-ionic strength of the mucosal surfaces allows the peptide to function as an efficient bactericidal barrier. In higher-salinity internal environments, the peptide likely maintains host protection through a dual-functional strategy, involving synergistic interactions with endogenous immune components and a functional transition toward immunomodulation. Beyond its natural role, Anguinin$_{55–72}$ holds significant biotechnological value as a valuable natural lead scaffold. Identifying its specific salt-sensitive threshold provides a critical baseline for rational molecular optimization. Future efforts could focus on enhancing its salt resistance by incorporating residues that promote hydrophobic-driven membrane insertion, such as substituting lysine with tryptophan or implementing bulky hydrophobic clusters to bypass the "charge-shielding" effect of electrolytes. Regarding thermal stability, Anguinin$_{55–72}$ maintained its antimicrobial effect against *S. epidermidis* and *A. baumannii* even following exposure to 100 °C for 30 min. This is comparable to other AMPs, such as BAMP, which also demonstrates excellent thermal stability [59]. This suggests that Anguinin$_{55–72}$ can maintain its antimicrobial activity in high-temperature conditions relevant to aquaculture applications. For example, when used as a feed additive, it may be exposed to high temperatures during production, transportation, storage, and application [60]. As reported, many AMPs exhibit cytotoxicity, such as LL-37, which can damage the cell membranes of human cells when its concentration is close to that required for exerting antimicrobial effects [61,62]. However, Anguinin$_{55–72}$ exhibited no cytotoxicity against HEK293T and ZF4 cells even at a concentration of 96 μM, a concentration well below its MIC, indicating its good biocompatibility and relatively safe for *in vivo* applications.

Finally, we evaluated the *in vivo* activity of Anguinin$_{55–72}$. Previous studies have indicated that AMPs not only possess direct antimicrobial effects but also significantly modulate immune responses *in vivo*, thereby facilitating the control of microbial infections within the host [63]. First, we used a zebrafish bacterial infection model to investigate whether Anguinin$_{55–72}$ has *in vivo* anti-infective properties. Subsequently, we further explored the *in vivo* efficacy against *E. tarda* within the Japanese eel. Similarly, treatment with Anguinin$_{55–72}$ significantly improved the survival rate of Japanese eels infected by *E. tarda*, reinforcing its

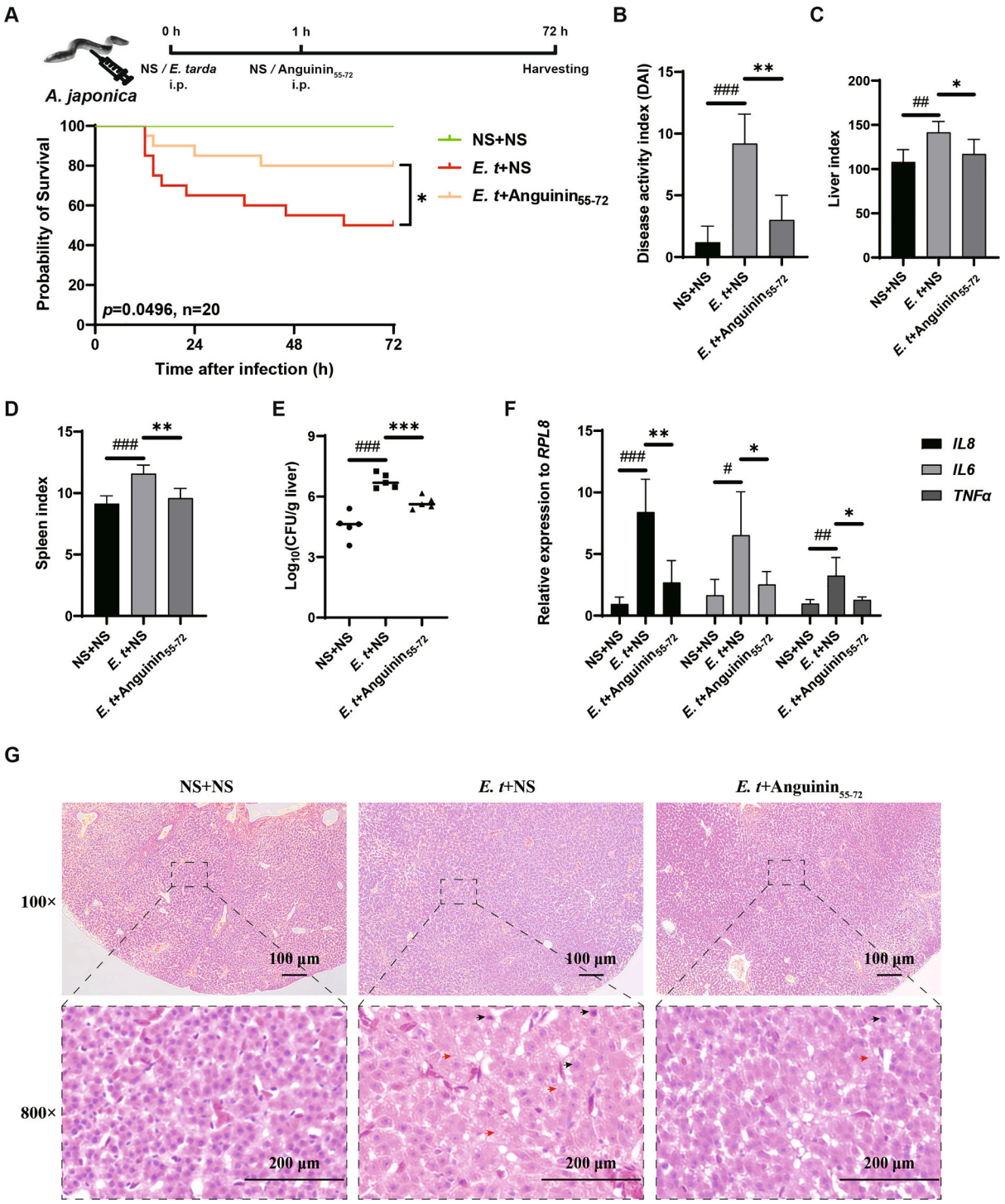

Fig. 9. Therapeutic efficacy of Anguinin$_{55–72}$ in *E. tarda*-infected Japanese eel. (A) Schematic representation of the infection protocol with *E. tarda* in Japanese eel and the corresponding survival curve (n = 20). Evaluation of the disease activity index (B), liver index (C) and spleen index (D). (E) Quantification of bacterial load in the liver of Japanese eel. (F) Expression analysis of inflammation-related genes in the liver of Japanese eel (n = 5). (G) Histopathological examination of liver sections stained with HE. Black arrows: Hepatocytes with nuclear contour deformation and nuclear hypertrophy; Red arrows: Cytoplasmic vacuolization. Statistical analysis was conducted through Student's *t*-test. #$p < 0.05$, ##$p < 0.01$, ###$p < 0.001$ indicated significant differences between blank group (NS + NS) and control group (*E. tarda* + NS). *$p < 0.05$, **$p < 0.01$, ***$p < 0.001$ indicated significant differences between control group (*E. tarda* + NS) and treatment group (*E. tarda* + Anguinin$_{55–72}$). (For interpretation of the references to colour in this figure legend, the reader is referred to the web version of this article.)

potential for the treatment of bacterial infections. Infection of Japanese eels with *E. tarda* led to severe systemic infections, and infected eels typically exhibited symptoms such as hepatomegaly, multifocal abscesses, and hemorrhagic ascites [46,64]. In this study, we observed reduction in disease activity index (DAI) and organ indices (liver and spleen) in Anguinin$_{55–72}$-treated eels, suggesting that the peptide can mitigates the systemic effect of infection. Furthermore, the bacterial load in the processed eel liver was significantly reduced. Interestingly, Anguinin$_{55–72}$ showed no significant antibacterial activity against *E. tarda in vitro*. This is similar to the previous study on Spasins$_{141–165}$,

which showed no significant antibacterial activity against *Aeromonas hydrophila in vitro* but was able to increase the survival rate of zebrafish infected with *Pseudomonas aeruginosa* by approximately 20% and reduce the bacterial load in the spleen [53]. One possible reason is that the antimicrobial peptides exert an immune regulatory effect in the body, assisting in killing bacteria by regulating the host's immune system [65,66]. Alternatively, it could be that Anguinin$_{55–72}$ is able to kill *E. tarda* in the body because the complex physiological environment inside the body is different from that *in vitro* [67]. It is also possible that both mechanisms are at play simultaneously. To clarify this issue, more in-depth research is needed.

Previous research has shown that fish can produce a range of cytokines that effectively engage with microbial invaders [68]. Specifically, pro-inflammatory cytokines play a crucial role in the immune regulation of fish [69]. *TNF-α*, *IL-1β*, *IL-6*, and *IL8* are essential components of the immune system that help to fight off pathogens and also play a significant role in the inflammatory response [70]. Infection of Japanese eel by *E. tarda* results in higher cell death rates and increased production of pro-inflammatory cytokines, such as *IL-6*, *IL-1β*, and TNF-α, leading to the disruption of immune homeostasis [71]. In our research, the downregulation of pro-inflammatory cytokines (*IL8*, *IL6*, and *TNFα*) in the liver of Anguinin$_{55–72}$-treated eels suggests that the peptide may also possess immunoregulatory properties, similar to those reported for other AMPs such as Epinecidin-1 and LLEL [54,72]. This dual action, antimicrobial and anti-inflammatory action, may be crucial in controlling infections, as it not only combats the pathogens, but also reduces the excessive inflammatory response that often contributes to disease pathology. Furthermore, after being infected by the *E. tarda*, the liver tissues of fish will show severe pathological changes. For example, in tilapia, after being infected by the *E. tarda*, there will be phenomena such as enlarged liver cells and aggregation of melanin macrophage centers (MMC) [73]. The histopathological examination of liver tissues in this study indicated that compared to the control group, Anguinin$_{55–72}$-treated eels exhibited substantial restoration of hepatocyte integrity, whereas the control group showed marked cellular damage. This indicates that Anguinin$_{55–72}$ may promote tissue repair and recovery, further supporting its potential as a comprehensive therapeutic agent.

Taken together, while Anguinin$_{55–72}$ belongs to the well-documented structural class of cationic α-helical AMPs, it possesses several distinct advantages that enhance its significance and therapeutic relevance. Unlike many representative α-helical peptides such as LL-37 or melittin, which are often limited by significant cytotoxicity and hemolytic activity at concentrations near their MICs, Anguinin$_{55–72}$ exhibits a remarkably high therapeutic index, maintaining cellular safety even at concentrations far exceeding its antimicrobial threshold (up to 96 μM). Furthermore, its multifaceted role—combining direct membrane disruption with potent immunomodulatory properties and the ability to promote tissue repair—sets it apart from traditional "pore-forming only" peptides. These characteristics, coupled with its exceptional thermal stability and demonstrated *in vivo* efficacy despite *in vitro* salt sensitivity, underscore Anguinin$_{55–72}$ as a specialized and highly effective defense molecule, offering distinct advantages for practical health management in the aquaculture industry.

5. Conclusions

In summary, we obtained a novel functional gene in Japanese eel and named it *Anguinin*. Based on the analysis of the physicochemical properties of Anguinin, we screened and identified a novel AMP, Anguinin$_{55–72}$, which exhibits broad-spectrum antimicrobial activity. Anguinin$_{55–72}$ can disrupt the cell membranes of bacteria, thereby increasing membrane permeability and inducing the accumulation of ROS, which ultimately leads to bacterial cell death. Furthermore, Anguinin$_{55–72}$ is capable of inhibiting and eliminating bacterial biofilms and exhibits excellent thermal stability and biocompatibility. Notably, treatment with Anguinin$_{55–72}$ observably improved the survival rate of zebrafish and Japanese eels infected with *E. tarda*, reduced the disease-related indices in Japanese eel, decreased liver bacterial loads, suppressed the expression of pro-inflammatory genes, and improved the pathological changes in liver tissues. Overall, the AMP Anguinin$_{55–72}$ holds great potential as a candidate for antibacterial infection treatment and has broad application prospects in aquaculture.

CRediT authorship contribution statement

Wenbin Zheng: Writing – original draft, Validation, Methodology, Investigation, Formal analysis, Data curation. **Fangyi Chen:** Writing – review & editing, Supervision, Project administration, Funding acquisition, Conceptualization. **Wenhao Yu:** Methodology, Investigation. **Tingting Gao:** Methodology, Investigation. **Ziyuan Yan:** Methodology, Investigation. **Yuqi Bai:** Investigation. **Hang Sun:** Investigation. **Ke-Jian Wang:** Writing – review & editing, Supervision, Project administration, Funding acquisition, Conceptualization.

Ethical approval

All fish experiments were authorized by the Experimental Animal Ethics Committee at Xiamen University, with the reference number XMULAC20240211, and were conducted in accordance with local regulations for research animal use.

Declaration of competing interest

The authors declare that they have no known competing financial interests or personal relationships that could have appeared to influence the work reported in this paper.

Acknowledgments

The work was supported by several grants, including the National Natural Science Foundation of China (grant numbers 42376089), Fujian Ocean and Fisheries Bureau (grant FJHYF-L-2025-13), Fujian Province Industry-Academia Collaboration Project (grant 2025N5001), and Xiamen Ocean Development Bureau (grant 22CZP002HJ08). Additionally, this work was supported by the PhD Fellowship of the State Key Laboratory of Marine Environmental Science at Xiamen University. We also appreciate laboratory engineers Hua Hao, Huiyun Chen, Ming Xiong, Zhiyong Lin and Hui Peng for their technical support.

Data availability

No data was used for the research described in the article.

References

[1] S.B. Park, T. Aoki, T.S. Jung, Pathogenesis of and strategies for preventing *Edwardsiella tarda* infection in fish, Vet. Res. 43 (2012) 67, https://doi.org/10.1186/1297-9716-43-67.

[2] T. Hoshina, On a new bacterium, Paracolobactrum anguillimortiferum n. sp, Nippon Suisan Gakkaishi 28 (1962) 162–164, https://doi.org/10.2331/suisan.28.162.

[3] M.X. Chen, M. Xu, Z.H. Chen, Q.J. Wan, S.L. Guo, Protective effects of OmpA exposure via *Bacillus subtilis* spore bathing on Japanese eel (*Anguilla japonica*) against *Edwardsiella anguillarum* infection, Aquaculture 586 (2024) 740771, https://doi.org/10.1016/j.aquaculture.2024.740771.

[4] A. Edrees, A.S.A. Abdel-Daim, N.S. Shaban, O. Shehata, R.E. Ibrahim, D dietary intervention of propolis and/or turmeric boosted growth, hematology, biochemical profile, and antioxidant-immune responses and their associated gene expression in Nile tilapia (*Oreochromis niloticus*) challenged with *Edwardsiella tarda*, Aquac. Int. 33 (2025) 46, https://doi.org/10.1007/s10499-024-01741-8.

[5] W.J. Jang, M.H. Jeon, S.J. Lee, S.Y. Park, Y.S. Lee, D. Noh, S.W. Hur, S. Lee, B. J. Lee, J.M. Lee, K.W. Kim, E.W. Lee, M.T. Hasan, Dietary supplementation of *Bacillus sp.* PM8313 with β-glucan modulates the intestinal microbiota of red sea bream (*Pagrus major*) to increase growth, immunity, and disease resistance, Front. Immunol. 13 (2022) 960554, https://doi.org/10.3389/fimmu.2022.960554.

[6] G.J. Yu, S.F. Zhao, W.H. Ou, Q.H. Ai, W.B. Zhang, K.S. Mai, Y.J. Zhang, Host-associated *Bacillus velezensis* T20 improved disease resistance and intestinal health of juvenile turbot (Scophthalmus maximus), Aquacult. Rep. 35 (2024) 101927, https://doi.org/10.1016/j.aqrep.2024.101927.

[7] A.R. Armwood, M.J. Griffin, B.M. Richardson, D.J. Wise, C. Ware, A.C. Camus, Pathology and virulence of *Edwardsiella tarda*, *Edwardsiella piscicida*, and *Edwardsiella anguillarum* in channel (*Ictalurus punctatus*), blue (*Ictalurus furcatus*), and channel × blue hybrid catfish, J. Fish Dis. 45 (2022) 1683–1698, https://doi.org/10.1111/jfd.13691.

[8] O.L.M. Haenen, H.T. Dong, T.D. Hoai, M. Crumlish, I. Karunasagar, T. Barkham, S. L. Chen, R. Zadoks, A. Kiermeier, B. Wang, E.G. Gamarro, M. Takeuchi, M.N. A. Azmai, B. Fouz, R. Pakingking Jr., Z.W. Wei, M.G. Bondad-Reantaso, Bacterial diseases of tilapia, their zoonotic potential and risk of antimicrobial resistance, Rev. Aquac. 15 (2023) 154–185, https://doi.org/10.1111/raq.12743.

[9] Z.y. Zeng, Z.l. Ding, A.n. Zhou, C.b. Zhu, S. Yang, H. Fei, Bacterial diseases in *Siniperca chuatsi*: status and therapeutic strategies, Vet. Res. Commun. 48 (2024) 3579–3592, https://doi.org/10.1007/s11259-024-10538-2.

[10] P.R. Lee, C. Lin, The antibiotic paradox: how the misuse of antibiotics destroys their curative powers, Int. Microbiol. 46 (2003) 603–604, https://doi.org/10.1353/pbm.2003.0088.

[11] S.K. Ahmed, S. Hussein, K. Qurbani, R.H. Ibrahim, A. Fareeq, K.A. Mahmood, M. G. Mohamed, Antimicrobial resistance: impacts, challenges, and future prospects, J. Med. Surg. Public Health 2 (2024) 100081, https://doi.org/10.1016/j.glmedi.2024.100081.

[12] N.S. Devi, R. Mythili, T. Cherian, R. Dineshkumar, G.K. Sivaraman, R. Jayakumar, M. Prathaban, M. Duraimurugan, V. Chandrasekar, W.J.G.M. Peijnenburg, Overview of antimicrobial resistance and mechanisms: the relative status of the past and current, Microbe 3 (2024) 100083, https://doi.org/10.1016/j.microb.2024.100083.

[13] M. Naddaf, 40 million deaths by 2050: toll of drug-resistant infections to rise by 70%, Nature 633 (2024) 747–748, https://doi.org/10.1038/d41586-024-03033-w.

[14] S.A. Kraemer, A. Ramachandran, G.G. Perron, Antibiotic pollution in the environment: from microbial ecology to public policy, Microorganisms 7 (2019) 180, https://doi.org/10.3390/microorganisms7060180.

[15] Y. Li, Q. Xiang, Q. Zhang, Y. Huang, Z. Su, Overview on the recent study of antimicrobial peptides: origins, functions, relative mechanisms and application, Peptides 37 (2012) 207–215, https://doi.org/10.1016/j.peptides.2012.07.001.

[16] N. Mookherjee, M.A. Anderson, H.P. Haagsman, D.J. Davidson, Antimicrobial host defence peptides: functions and clinical potential, Nat. Rev. Drug Discov. 19 (2020) 311–332, https://doi.org/10.1038/s41573-019-0058-8.

[17] S. Omardien, S. Brul, S.A.J. Zaat, Antimicrobial activity of cationic antimicrobial peptides against gram-positives: current progress made in understanding the mode of action and the response of bacteria, Front. Cell Dev. Biol. 4 (2016) 111, https://doi.org/10.3389/fcell.2016.00111.

[18] P. Kumar, J.N. Kizhakkedathu, S.K. Straus, Antimicrobial peptides: diversity, mechanism of action and strategies to improve the activity and biocompatibility *in vivo*, Biomolecules 8 (2018) 4, https://doi.org/10.3390/biom8010004.

[19] D.E. Fry, Antimicrobial peptides, Surg. Infect. 19 (2018) 804–811, https://doi.org/10.1089/sur.2018.194.

[20] K.E. Greber, M. Roch, M.A. Rosato, M.P. Martinez, A.E. Rosato, Efficacy of newly generated short antimicrobial cationic lipopeptides against methicillin-resistant *Staphylococcus aureus* (MRSA), Int. J. Antimicrob. Agents 55 (2020) 105827, https://doi.org/10.1016/j.ijantimicag.2019.10.008.

[21] X. Li, S.Y. Zuo, B. Wang, K.Y. Zhang, Y. Wang, Antimicrobial mechanisms and clinical application prospects of antimicrobial peptides, Molecules 27 (2022) 2675, https://doi.org/10.3390/molecules27092675.

[22] Y.H. Yan, Y.Z. Li, Z.W. Zhang, X.H. Wang, Y.Z. Niu, S.H. Zhang, W.L. Xu, C.G. Ren, Advances of peptides for antibacterial applications, Colloids Surf. B: Biointerfaces 202 (2021) 111682, https://doi.org/10.1016/j.colsurfb.2021.111682.

[23] K. Browne, S. Chakraborty, R.X. Chen, M.D.P. Willcox, D.S. Black, W.R. Walsh, N. Kumar, A new era of antibiotics: the clinical potential of antimicrobial peptides, Int. J. Mol. Sci. 21 (2020) 7047, https://doi.org/10.3390/ijms21197047.

[24] A.O. Kordon, A. Karsi, L. Pinchuk, Innate immune responses in fish: antigen presenting cells and professional phagocytes, Turk. J. Fish. Aquat. Sci. 18 (2018) 1123–1139, https://doi.org/10.4194/1303-2712-v18_9_11.

[25] Y. Liang, R.Z. Guan, W.S. Huang, T.L. Xu, Isolation and identification of a novel inducible antibacterial peptide from the skin mucus of Japanese eel, *Anguilla japonica*, Protein J. 30 (2011) 413–421, https://doi.org/10.1007/s10930-011-9346-9.

[26] D.L. Zhang, R.Z. Guan, W.S. Huang, J. Xiong, Isolation and characterization of a novel antibacterial peptide derived from hemoglobin alpha in the liver of Japanese eel, *Anguilla japonica*, Fish Shellfish Immunol. 35 (2013) 625–631, https://doi.org/10.1016/j.fsi.2012.08.022.

[27] Q. Li, S.S. Li, S.W. Li, X.M. Hao, A.Q. Wang, S.Y. Si, Y.N. Xu, J.C. Shu, M.L. Gan, Antimicrobial and anti-inflammatory cyclic tetrapeptides from the co-cultures of two marine-derived fungi, J. Nat. Prod. 87 (2024) 365–370, https://doi.org/10.1021/acs.jnatprod.3c01115.

[28] W.L. Qiu, F.Y. Chen, R.S. Chen, S. Li, X.W. Zhu, M. Xiong, K.J. Wang, A new C-type lectin homolog SpCTL6 exerting immunoprotective effect and regulatory role in mud crab *Scylla paramamosain*, Front. Immunol. 12 (2021) 661823, https://doi.org/10.3389/fimmu.2021.661823.

[29] W.S. Huang, Z.X. Wang, Y. Liang, P. Nie, B. Huang, Characterization of MyD88 in Japanese eel, *Anguilla japonica*, Fish Shellfish Immunol. 81 (2018) 374–382, https://doi.org/10.1016/j.fsi.2018.07.028.

[30] T.T. Priyathilaka, Y. Kim, H.M.V. Udayantha, S. Lee, H.M.L.P.B. Herath, H.H. C. Lakmal, D.A.S. Elvitigala, N. Umasuthan, G.I. Godahewa, S.I. Kang, H.B. Jeong, S.K. Kim, D.J. Kim, B.S. Lim, Identification and molecular characterization of peroxiredoxin 6 from Japanese eel (*Anguilla japonica*) revealing its potent antioxidant properties and putative immune relevancy, Fish Shellfish Immunol. 51 (2016) 291–302, https://doi.org/10.1016/j.fsi.2015.12.012.

[31] K.J. Livak, T.D. Schmittgen, Analysis of relative gene expression data using real-time quantitative PCR and the $2^{-\Delta\Delta CT}$ method, Methods 25 (2001) 402–408, https://doi.org/10.1006/meth.2001.1262.

[32] Z.G. Shan, K.X. Zhu, H. Peng, B. Chen, J. Liu, F.Y. Chen, X.W. Ma, S.P. Wang, K. Qiao, K.J. Wang, The new antimicrobial peptide SpHyastatin from the mud crab *Scylla paramamosain* with multiple antimicrobial mechanisms and high effect on bacterial infection, Front. Microbiol. 7 (2016) 1140, https://doi.org/10.3389/fmicb.2016.01140.

[33] Y.Q. Bai, W.B. Zhang, W.B. Zheng, X.Z. Meng, Y.Y. Duan, C. Zhang, F.Y. Chen, K. J. Wang, A 14-amino acid cationic peptide Bolespleenin$_{334\text{-}347}$ from the marine fish mudskipper *Boleophthalmus pectinirostris* exhibiting potent antimicrobial activity and therapeutic potential, Biochem. Pharmacol. 226 (2024) 116344, https://doi.org/10.1016/j.bcp.2024.116344.

[34] X.F. Wang, X. Hong, F.Y. Chen, K.J. Wang, A truncated peptide Spgillcin$_{177\text{-}189}$ derived from mud crab *Scylla paramamosain* exerting multiple antibacterial activities, Front. Cell. Infect. Microbiol. 12 (2022) 928220, https://doi.org/10.3389/fcimb.2022.928220.

[35] X.W. Zhu, F.Y. Chen, S. Li, H. Peng, K.J. Wang, A novel antimicrobial peptide Sparanegtin identified in *Scylla paramamosain* showing antimicrobial activity and immunoprotective role *in vitro* and *vivo*, Int. J. Mol. Sci. 23 (2022) 15, https://doi.org/10.3390/ijms23010015.

[36] W.B. Zhang, Z. An, Y.Q. Bai, Y. Zhou, F.Y. Chen, K.J. Wang, A novel antimicrobial peptide Scyreptin$_{1\text{-}30}$ from *Scylla paramamosain* exhibiting potential therapy of *Pseudomonas aeruginosa* early infection in a mouse burn wound model, Biochem. Pharmacol. 218 (2023) 115917, https://doi.org/10.1016/j.bcp.2023.115917.

[37] X. Wang, X. Zhao, M. Malik, K. Drlica, Contribution of reactive oxygen species to pathways of quinolone-mediated bacterial cell death, J. Antimicrob. Chemother. 65 (2010) 520–524, https://doi.org/10.1093/jac/dkp486.

[38] Y. Yang, F.Y. Chen, H.Y. Chen, H. Peng, H. Hao, K.J. Wang, A novel antimicrobial peptide Scyreprocin from mud crab *Scylla paramamosain* showing potent antifungal and anti-biofilm activity, Front. Microbiol. 11 (2020) 1589, https://doi.org/10.3389/fmicb.2020.01589.

[39] Y.C. Chen, Y. Yang, C. Zhang, H.Y. Chen, F.Y. Chen, K.J. Wang, A novel antimicrobial peptide Sparamosin$_{26\text{-}54}$ from the mud crab *Scylla paramamosain* showing potent antifungal activity against *Cryptococcus neoformans*, Front. Microbiol. 12 (2021) 746006, https://doi.org/10.3389/fmicb.2021.746006.

[40] N. Malanovic, K. Lohner, Gram-positive bacterial cell envelopes: the impact on the activity of antimicrobial peptides, Biochim. Biophys. Acta Biomembr. 1858 (2016) 936–946, https://doi.org/10.1016/j.bbamem.2015.11.004.

[41] J.T.A. Oliveira, P.F.N. Souza, I.M. Vasconcelos, L.P. Dias, T.F. Martins, M.F. Van Tilburg, M.I.F. Guedes, D.O.B. Sousa, Mo-CBP3-PepI, Mo-CBP3-PepII, and Mo-CBP3-PepIII are synthetic antimicrobial peptides active against human pathogens by stimulating ROS generation and increasing plasma membrane permeability, Biochimie 157 (2019) 10–21, https://doi.org/10.1016/j.biochi.2018.10.016.

[42] A. Rajput, A. Thakur, S. Sharma, M. Kumar, aBiofilm: a resource of anti-biofilm agents and their potential implications in targeting antibiotic drug resistance, Nucleic Acids Res. 46 (2018) D894–D900, https://doi.org/10.1093/nar/gkx1157.

[43] S.K. Singh, M.M. Meitei, T.G. Choudhary, N. Soibam, P. Biswas, G. Waikhom, Chapter 15 - bacterial diseases in cultured fishes: An update of advances in control measures, in: Bacterial Fish Diseases, Academic Press, 2022, pp. 307–335.

[44] T. Qi, S. Wei, Z. Li, L. Ribas, Q. Cao, Current research on bacterial diseases in eel: An immunological perspective, Aquaculture 595 (2025) 741599, https://doi.org/10.1016/j.aquaculture.2024.741599.

[45] T.T. Xu, X.H. Zhang, *Edwardsiella tarda*: an intriguing problem in aquaculture, Aquaculture 431 (2014) 129–135, https://doi.org/10.1016/j.aquaculture.2013.12.001.

[46] W.J. Jung, J. Kwon, S.S. Giri, S.G. Kim, S.W. Kim, J.W. Kang, S.B. Lee, Y.M. Lee, W. T. Oh, J.W. Jun, S.C. Park, Isolation and characterization of a highly virulent *Edwardsiella piscicida* strain responsible for mass mortality in marbled eel (*Anguilla marmorata*) cultured in Korea, Aquaculture 555 (2022) 738199, https://doi.org/10.1016/j.aquaculture.2022.738199.

[47] M.G. Bondad-Reantaso, B. MacKinnon, I. Karunasagar, S. Fridman, V. Alday-Sanz, E. Brun, M. Le Groumellec, A. Li, W. Surachetpong, I. Karunasagar, B. Hao, A. Dall'Occo, R. Urbani, A. Caputo, Review of alternatives to antibiotic use in aquaculture, Rev. Aquac. 15 (2023) 1421–1451, https://doi.org/10.1111/raq.12786.

[48] H.X. Li, J.H. Niu, X.L. Wang, M.F. Niu, C.S. Liao, The contribution of antimicrobial peptides to immune cell function: A review of recent advances, Pharmaceutics 15 (2023) 2278, https://doi.org/10.3390/pharmaceutics15092278.

[49] N.C. Smith, M.L. Rise, S.L. Christian, A comparison of the innate and adaptive immune systems in cartilaginous fish, ray-finned fish, and lobe-finned fish, Front. Immunol. 10 (2019) 2292, https://doi.org/10.3389/fimmu.2019.02292.

[50] P.R. Rauta, B. Nayak, S. Das, Immune system and immune responses in fish and their role in comparative immunity study: A model for higher organisms, Immunol. Lett. 148 (2012) 23–33, https://doi.org/10.1016/j.imlet.2012.08.003.

[51] M. Islam, F. Asif, S.U. Zaman, K.H. Arnab, M. Rahman, M. Hasan, Effect of charge on the antimicrobial activity of alpha-helical amphibian antimicrobial peptide, Curr. Res. Microb. Sci. 4 (2023) 100182, https://doi.org/10.1016/j.crmicr.2023.100182.

[52] B.L. Huy, H.B.T. Phuong, B.N.T. Thanh, Q.T. Van, H.V. Dinh, H.L. Xuan, Influence of hydrophobicity on the antimicrobial activity of helical antimicrobial peptides: a study focusing on three mastoparans, Mol. Divers. (2024) 1–8, https://doi.org/10.1007/s11030-024-11046-w.
[53] C. Zhang, F.Y. Chen, Y.Q. Bai, X.X. Dong, X.Z. Meng, K.J. Wang, A novel antimicrobial peptide Spasin$_{141-165}$ identified from *Scylla paramamosain* exhibiting protection against *Aeromonas hydrophila* infection, Aquaculture 591 (2024) 741137, https://doi.org/10.1016/j.aquaculture.2024.741137.
[54] J.L. Narayana, H.N. Huang, C.J. Wu, J.Y. Chen, Epinecidin-1 antimicrobial activity: *in vitro* membrane lysis and *in vivo* efficacy against *helicobacter pylori* infection in a mouse model, Biomaterials 61 (2015) 41–51, https://doi.org/10.1016/j.biomaterials.2015.05.014.
[55] Z.L. He, Q. Xu, B. Newland, R. Foley, I. Lara-Saez, J.F. Curtin, W.X. Wang, Reactive oxygen species (ROS): utilizing injectable antioxidative hydrogels and ROS-producing therapies to manage the double-edged sword, J. Mater. Chem. B 9 (2021) 6326–6346, https://doi.org/10.1039/d1tb00728a.
[56] B. Lee, J.S. Hwang, D.G. Lee, Antibacterial action of lactoferricin B like peptide against *Escherichia coli*: reactive oxygen species-induced apoptosis-like death, J. Appl. Microbiol. 129 (2020) 287–295, https://doi.org/10.1111/jam.14632.
[57] H. Nikaido, Molecular basis of bacterial outer membrane permeability revisited, Microbiol. Mol. Biol. Rev. 67 (2003) 593, https://doi.org/10.1128/MMBR.67.4.593-656.2003.
[58] G. Batoni, G. Maisetta, S. Esin, Therapeutic potential of antimicrobial peptides in polymicrobial biofilm-associated infections, Int. J. Mol. Sci. 22 (2021) 482, https://doi.org/10.3390/ijms22020482.
[59] S. Choyam, P.M. Jain, R. Kammara, Characterization of a potent new-generation antimicrobial peptide of *Bacillus*, Front. Microbiol. 12 (2021) 710741, https://doi.org/10.3389/fmicb.2021.710741.
[60] Z.H. Su, H.J. Yu, T.T. Lv, Q.Z. Chen, H. Luo, H.T. Zhang, Progress in the classification, optimization, activity, and application of antimicrobial peptides, Front. Microbiol. 16 (2025) 1582863, https://doi.org/10.3389/fmicb.2025.1582863.
[61] D.M.E. Bowdish, D.J. Davidson, Y.E. Lau, K. Lee, M.G. Scott, R.E.W. Hancock, Impact of LL-37 on anti-infective immunity, J. Leukoc. Biol. 77 (2005) 451–459, https://doi.org/10.1189/jlb.0704380.
[62] K. Chen, W. Gong, J. Huang, T. Yoshimura, J.M. Wang, The potentials of short fragments of human anti-microbial peptide LL-37 as a novel therapeutic modality for diseases, Front. Biosci.-Landmark 26 (2021) 1362–1372, https://doi.org/10.52586/5029.
[63] J.H. Ouyang, Y.Y. Zhu, W.J. Hao, X. Wang, H.X. Yang, X.Y. Deng, T.T. Feng, Y. Huang, H.I. Yu, Y.P. Wang, Three naturally occurring host defense peptides protect largemouth bass (*Micropterus salmoides*) against bacterial infections, Aquaculture 546 (2022) 737383, https://doi.org/10.1016/j.aquaculture.2021.737383.
[64] T. Fujii, M. Yoshikawa, N. Kondo, S. Yamakawa, K. Funasaka, Y. Hirooka, T. Tochio, Synbiotic administration in Japanese eels with prebiotic 1-kestose and probiotic *Lactiplantibacillus plantarum* FM8 improved feed efficiency and significantly reduced the levels of *Edwardsiella*, Fish. Sci. 90 (2024) 115–122, https://doi.org/10.1007/s12562-023-01739-w.
[65] Y. Luo, Y.Z. Song, Mechanism of antimicrobial peptides: antimicrobial, anti-inflammatory and antibiofilm activities, Int. J. Mol. Sci. 22 (2021) 11401, https://doi.org/10.3390/ijms222111401.
[66] S.C. Mansour, O.M. Pena, R.E.W. Hancock, Host defense peptides: front-line immunomodulators, Trends Immunol. 35 (2014) 443–450, https://doi.org/10.1016/j.it.2014.07.004.
[67] M.S. Zharkova, D.S. Orlov, O.Y. Golubeva, O.B. Chakchir, I.E. Eliseev, T. M. Grinchuk, O.V. Shamova, Application of antimicrobial peptides of the innate immune system in combination with conventional antibiotics-a novel way to combat antibiotic resistance? Front. Cell. Infect. Microbiol. 9 (2019) 128, https://doi.org/10.3389/fcimb.2019.00128.
[68] C. Secombes, Will advances in fish immunology change vaccination strategies? Fish Shellfish Immunol. 25 (2008) 409–416, https://doi.org/10.1016/j.fsi.2008.05.001.
[69] K.J. Laing, T.H. Wang, J. Zou, J. Holland, S.H. Hong, N. Bols, I. Hirono, T. Aoki, C. J. Secombes, Cloning and expression analysis of rainbow trout *Oncorhynchus mykiss* tumour necrosis factor-α, Eur. J. Biochem. 268 (2001) 1315–1322, https://doi.org/10.1046/j.1432-1327.2001.01996.x.
[70] P.A. Darrah, M.K. Hondalus, Q.P. Chen, H. Ischiropoulos, D.M. Mosser, Cooperation between reactive oxygen and nitrogen intermediates in killing of *Rhodococcus equi* by activated macrophages, Infect. Immun. 68 (2000) 3587–3593, https://doi.org/10.1128/IAI.68.6.3587-3593.2000.
[71] B.T. Birhanu, J.S. Lee, S.J. Lee, S.H. Choi, M.A. Hossain, J.Y. Park, J.C. Kim, J. W. Suh, S.C. Park, Immunomodulation of *lactobacillus pentosus* PL11 against *Edwardsiella tarda* infection in the head kidney cells of the Japanese eel (*Anguilla japonica*), Fish Shellfish Immunol. 54 (2016) 466–472, https://doi.org/10.1016/j.fsi.2016.04.023.
[72] L. Yuan, Q. Chu, B. Yang, W. Zhang, Q.C. Sun, R.C. Gao, Purification and identification of anti-inflammatory peptides from sturgeon (*Acipenser schrenckii*) cartilage, Food Sci. Human Wellness 12 (2023) 2175–2183, https://doi.org/10.1016/j.fshw.2023.03.030.
[73] N. Pinto, M.U. Nissa, M.A. Pathan, B.S. Yashwanth, M.G. Pratapa, S. Srivastava, M. Goswami, High throughput proteomic analysis of *Labeo rohita* liver infected with *Edwardsiella tarda*, Aquaculture 569 (2023) 739338, https://doi.org/10.1016/j.aquaculture.2023.739338.